

Chapter 1

Absolute and Relative Gravimetry

Ludger Timmen

Contents

1.1	Introduction	2
1.2	Characteristics of Absolute Gravimetry	2
1.2.1	General Aspects	2
1.2.2	Objectives of Geo-scientific and State-geodetic Surveys	3
1.3	Measurements with Free-Fall Absolute Gravimeters	5
1.3.1	Principles of FG5 Gravimeters	6
1.3.2	Observation Equation	7
1.3.3	Operational Procedures with FG5-220	9
1.3.4	Accuracy and Instrumental Offset	12
1.4	Relative Gravimetry	18
1.4.1	Principles of Spring Gravimeters	19
1.4.2	Observation Equation	21
1.4.3	Regional and Local Surveys with Scintrex SC-4492	22
1.4.4	Microgravimetric Measurements	26
1.4.5	Instrumental Drift	28
1.5	Reduction of Non-tectonic Gravity Variations	30
1.5.1	Earth's Body and Ocean Tides	31
1.5.2	Polar Motion	34
1.5.3	Atmospheric Mass Movements	37
1.5.4	Groundwater Variations	38
1.6	Gravity Changes: Examples	39
1.6.1	Hydrology: Groundwater Variations in Hannover	39
1.6.2	Tectonics: Isostatic Land Uplift in Fennoscandia	40
	References	43

L. Timmen (✉)

Institut für Erdmessung (IfE), Leibniz Universität Hannover (LUH), Schneiderberg 50, 30167 Hannover, Germany

e-mail: timmen@ife.uni-hannover.de

1.1 Introduction

Absolute and relative gravimetry allow the determination of gravity acceleration, usually just called gravity, for specific positions as well as the detection of gravity changes with time at a given location. For high-accuracy demands, the geometrical position of a gravity point has to be defined very accurately, e.g. in geodynamic research projects, at a height along the vertical above a ground mark. Geodetic networks with local, regional or global extent can be surveyed to monitor short-term and long-term gravity variations.

This chapter refers particularly to experience gained at the Institut für Erdmessung (IfE), Leibniz Universität Hannover (LUH). In the following, an overview of relative and absolute gravimetry (instrumental techniques, observation equations, accuracies, etc.) is given. Exemplarily for present state-of-the-art absolute and relative gravimeters, the main characteristics and accuracy estimates for the Hannover instruments are presented.

Because of the dynamics within the Earth's system (tectonics, climate change, sea-level rise), the national and international base networks are not stable with time. With the high accuracies of modern geodetic techniques, combined with the high quality of the base net stations (stable environment, customised facilities), the networks serve more and more as control systems for environmental changes and surface deformations.

The recommended unit of acceleration in the *Système International d'Unités* (SI) is the unit m/s^2 (BIPM 2006). In geodesy and geophysics, the non-SI unit Gal ($1 \text{ Gal} = 1 \text{ cm/s}^2 = 0.01 \text{ m/s}^2$) is also used to express acceleration due to gravity. In order to provide gravity differences and to describe small deviations or uncertainties of the measurements, the following units are helpful:

$$1 \text{ mGal} = 10^{-5} \text{ m/s}^2 = 10^{-6} g \quad \text{and} \quad 1 \mu\text{Gal} = 10^{-8} \text{ m/s}^2 = 10^{-9} g. \quad (1)$$

1.2 Characteristics of Absolute Gravimetry

1.2.1 General Aspects

To realise the advantages of absolute gravimetric measurements, some particular features of the gravity acceleration g , usually just called gravity g , for a defined geometrical point should be explained first. The gravity acceleration at a surface point depends on the following:

1. The position relative to the Earth's masses and their density distribution (integral effect caused by the gravitational force of the Earth's masses)
2. The position relative to the Earth's rotation axis (effect caused by the centrifugal force due to the Earth's rotation)

The g -value of a point at the Earth's surface (e.g. bench mark attached to a pier) changes with the following:

- Varying distance to the centre of masses of the Earth (geocentre) caused by vertical movements of the measuring point, e.g. due to crustal deformations, and by secular variations of the position of the geocentre (subtle effect, requires long-time measuring series)
- Mass shifts and redistributions within the system Earth (including atmosphere and hydrosphere) and especially with near-surface variations within the crust (e.g. groundwater changes, sediment compaction)
- Changing distance to the Earth's rotation pole due to lateral movements (subtle effect, e.g. due to plate tectonics)

Absolute gravity measurements are most sensitive to height changes and provide an obvious way to define and control the vertical height datum. No additional reference points (connection points) at the Earth's surface and no observations of celestial bodies (quasars, stars, planets, moon) or satellites are needed. Shortcomings of relative gravimetry, like calibration problems and deficiencies in the datum level definition, can be overcome. The accuracy of an absolute gravity net is independent of geographical extension which allows applications on local, regional and global scales with consistent measurement quality. An independent verification of displacements measured geometrically with GPS (Global Positioning System), VLBI (Very Long Baseline Interferometry) and SLR (Satellite Laser Ranging) is possible. A combination of gravimetric and geometric measurements may enable discrimination among subsurface mass movements associated with or without a surface deformation.

1.2.2 Objectives of Geo-scientific and State-geodetic Surveys

The benefit of absolute gravimetry has already been exploited in different scientific projects. The International Absolute Gravity Basestation Network (IAGBN) serves, among other purposes, for the determination of large-scale tectonic plate movements (Boedecker and Fritzer 1986; Boedecker and Flury 1995). The recommendations of the Interunion Commission on the Lithosphere on mean sea level and tides propose the regular implementation of absolute gravity measurements at coastal points, 1–10 km away from tide gauges (Carter et al. 1989). The height differences between gravity points and tide gauges have to be controlled by levelling or GPS. In Great Britain, the main tide gauges are controlled by repeated absolute gravity determinations in combination with episodic or continuous GPS measurements (Williams et al. 2001). Torge (1998a, b) describes the changing role of gravity reference networks due to the modern approach to realising the network standards by absolute observations.

Overall, absolute gravimetry can be an important research tool for studying geodynamic processes, especially land uplift effects due to postglacial rebound

(PGR). Lambert et al. (1996) give an overview of the capability of absolute gravity measurements in determining the temporal variations in the Earth's gravity field. In Lambert et al. (2001), the gravimetric results for the research of the Laurentide post-glacial rebound in Canada are described. Mäkinen et al. (2007) compare observed gravity changes in Antarctica with modelled predictions of the glacial isostatic adjustment as well as of the glacier mass balance.

Since 1986, several gravimetric projects were performed by IfE with the absolute gravimeters JILA_g-3 (e.g. Torge 1990, 1993; Timmen 1996) and FG5-220 (Gittlein et al. 2008; Timmen et al. 2006a). These activities served the following main objectives:

- Establishing and improving international and national gravity reference networks to realise a homogeneous gravity standard (datum definition in level and scale) of regional to global extent; calibration systems for relative gravimetry are needed
- Installing and strengthening regional and local networks in tectonically active areas with absolute gravimetric measurements and following re-observations; such monitoring systems may serve for geophysical research on the mechanism of crust formation and on the rheology of Earth's mantle and crust
- Monitoring the vertical stability of tide gauge stations to separate sea-level changes from land surface shifts; this serves to constrain parameters related to global climatic change

With the initiation of the GRACE satellite experiment (Gravity Recovery and Climate Experiment, e.g. Wahr and Velicogna 2003; Tapley et al. 2004), a new requirement has arisen for absolute gravimetry:

- To provide the most accurate “ground truth” for GRACE

The results from both data sets describe changes of the gravity field at the Earth's surface or at the geoid. The terrestrial data can not only be used to validate the GRACE products (Müller et al. 2006) but may also serve as a completion of the satellite results.

In the future, two additional tasks may become important applications:

- Monitoring of human-caused changes in aquifers and deep water reservoirs by water extraction
- Contributing to the definition of ground-based geodetic reference networks within the activities for the Global Geodetic Observing Systems (GGOS) of the International Association of Geodesy (IAG)

GGOS will provide the observational basis to integrate the different geodetic techniques. The purpose of the globally collected geodetic data is to collate and

analyse information about global processes and changes which are important for world societies. An overview and further details about GGOS can be obtained from Pearlman et al. (2006). In Ilk et al. (2005), detailed information about mass transport processes in the Earth system is given.

1.3 Measurements with Free-Fall Absolute Gravimeters

In January 1986, the Institut für Erdmessung (IfE), Leibniz Universität Hannover (LUH), received the absolute gravimeter JILAg-3 which was the first transportable system located in Germany (Torge et al. 1987). The free-fall system was developed at the Joint Institute of Laboratory Astrophysics (JILA, Faller et al. 1983) of the University of Colorado. The so-called JILAg-3 was the third gravimeter of a series of six JILA instruments and was successfully employed by IfE in more than 130 absolute gravity determinations at about 80 different stations (South America, China, Greenland, Iceland, central and northern Europe). In December 2002, IfE had received a new FG5 absolute gravity meter (FG5-220) from Micro-g Solutions, Inc. (now Micro-g LaCoste, Inc., Erie, Colorado), which was a state-of-the-art instrument (Niebauer et al. 1995) and replaced the older JILAg-3. Based on the JILA design, the FG5 generation has overcome several constructively pre-defined shortcomings and represents an essential improvement in operation and accuracy. The first fully operational FG5 instrument (FG5-101) was already available in 1993, manufactured by AXIS Instruments Company in Boulder, CO (Carter et al. 1994). The achievement of AXIS became possible after the National Institute of Standards and Technology (NIST, Boulder, USA) and the former Institute of Applied Geodesy (IfAG, now Federal Agency for Cartography and Geodesy, BKG, Frankfurt, Germany) joined forces in 1990 to produce an advanced instrument capable of providing more stringent data constraints on geophysical investigations.

The FG5 series represents the currently most advanced instruments and has to be assumed as the best instrumental realisation to measure the absolute gravity acceleration. Besides the FG5 meter for most accurate applications, a portable absolute gravimeter for harsh field environments has been developed by Micro-g LaCoste, Inc., called A10 (Niebauer et al. 1999, see also the Micro-g LaCoste internet pages). This unique instrument allows a data sampling rate of 1 Hz and provides a precision of $10 \mu\text{Gal}$ after 10 min of measurements at a quiet outdoor field site. An absolute accuracy of $10 \mu\text{Gal}$ can be achieved for a station determination. Liard and Gagnon (2002) tested their new A10 in 2001 at the International Comparison of Absolute Gravimeters in Sèvres, France. The investigations of Schmerge and Francis (2006) confirm the accuracy specifications of the manufacturer.

Figure 1.1 shows the two types of the Hannover absolute gravimeters, the instruments JILAg-3 and FG5-220. During the period from 1986 to 2000, the JILAg-3 gravimeter was used by IfE for absolute gravity determinations on more than 80 different sites worldwide. The measurements with the presently employed FG5-220

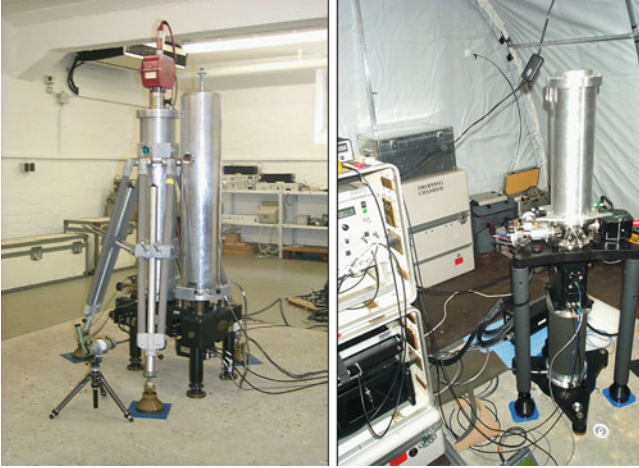


Fig. 1.1 The two absolute gravimeters of the Leibniz Universität Hannover: *left* JILAg-3 employed from 1986 to 2000 (here reference measurements in Hannover), *right* FG5-220 operated since 2003 (tent measurements in Denmark)

started in 2003, and more than 40 different sites in central and northern Europe have already been visited.

1.3.1 Principles of FG5 Gravimeters

Modern absolute gravity measurements are based on time and distance measurements along the vertical to derive the gravity acceleration at a specific position on the Earth, cf. Torge (1989). The expression “absolute” is based on the fact that the time and length standards (rubidium clock, helium–neon laser) are incorporated as components of the gravimeter system. No external reference like a connecting point is required. The FG5 series is presently the most common gravimeter model, which may be considered as the successor system of the JILA generation (Carter et al. 1994; Niebauer et al. 1995). The influence of floor vibration and tilt on the optical path could largely be removed by the improved interferometer design. The iodine-stabilised laser, serving as the primary length standard, is separated from the instrumental vibrations, caused by the free-fall experiments (drops), by routing the laser light through a fibre optic cable to the interferometer base; see Fig. 1.2.

During a drop, the trajectory of a test mass (optical retro-reflector) is traced by laser interferometry over the falling distance of about 20 cm within an evacuated chamber. The “co-falling” drag-free cart provides a molecular shield for the dropped object. The multiple time–distance data pairs collected during the drop (FG5: 700 pairs at equally spaced measuring positions, JILAg: 200) are adjusted to a fitting curve (almost parabolic) as shown in Fig. 1.3, giving the gravity acceleration g for the reference height above floor level (FG5: ~ 1.2 m, JILAg: ~ 0.8 m).

Fig. 1.2 Schematic diagram of the FG5 absolute gravimeter, after Micro-g Solutions, Inc. (1999), courtesy of Micro-g Lacoste, Inc.

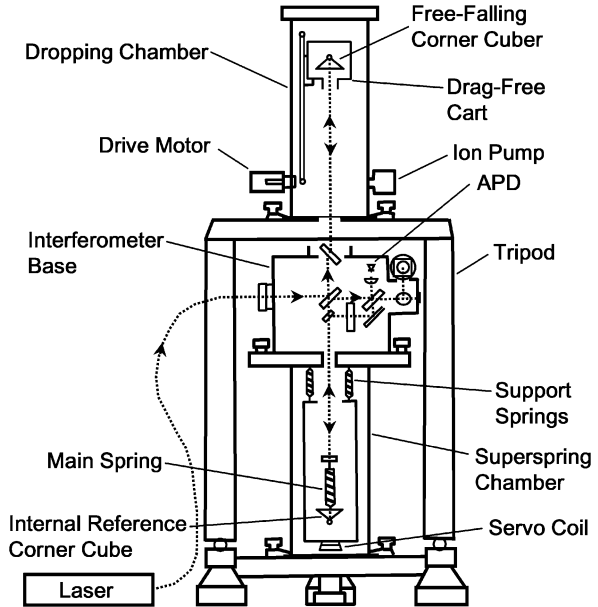
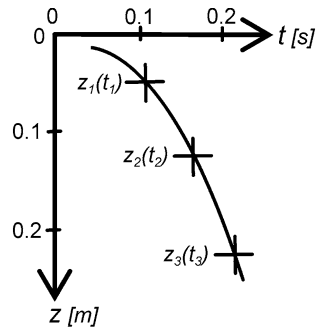


Fig. 1.3 The free-fall in a time–distance diagram



1.3.2 Observation Equation

In a uniform gravity field, the motion of a freely falling mass m can be expressed with the following equation of motion:

$$m \frac{d^2z}{dt^2} = m \ddot{z} = m g. \tag{2}$$

Figure 1.3 shows the time–distance diagram with the axis t and z where the z -axis coincides with the direction of gravity. Eliminating m in (2), the integration yields an equation for the velocity

$$\dot{z} = \dot{z}_0 + g t, \quad \text{with } \dot{z}_0 = v_0, \quad (3)$$

and thereafter for the position

$$z = z_0 + v_0 t + \frac{g}{2} t^2 \quad (4)$$

of a body during a free fall. The initial parameters, displacement z_0 and velocity v_0 , are adjustment unknowns valid at the time $t = 0$. For most accurate gravity determination, the non-uniformity of the Earth's gravitational field has to be taken into account. Along the plumb line, the gravity acceleration g varies with height. This can be considered as a linear gravity change along the free-fall trajectory during an experiment with an absolute gravimeter. Hence formula (2) is extended with a constant vertical gravity gradient γ :

$$m\ddot{z} = m(g_0 + \frac{dg}{dz}z) = m(g_0 + \gamma z). \quad (5)$$

The acceleration g_0 is defined for the position $z = 0$ which is, in common practice with FG5 and JILA meters, the resting position of the gravity centre of the test mass at the start of the free-fall experiment ("top-of-the-drop"). Neglecting the initial parameters and double integration of (5) gives (Cook 1965)

$$z = \frac{g_0}{\gamma}(\cosh \gamma^{1/2} t - 1), \quad \text{with } z_0 = v_0 = 0. \quad (6)$$

Because the initial parameters z_0 and v_0 have to be included, the variable z is expanded to the power series

$$z = f(t) = c_0 + c_1(t - t_0) + c_2(t - t_0)^2 + c_3(t - t_0)^3 + \dots \quad (7)$$

With $t_0 = 0$ the following equations are deduced:

$$z = c_0 + c_1 t + c_2 t^2 + c_3 t^3 + \dots, \quad z(t=0) = c_0 \Rightarrow c_0 = z_0, \quad (8)$$

$$\dot{z} = c_1 + 2c_2 t + 3c_3 t^2 + \dots, \quad \dot{z}(t=0) = c_1 \Rightarrow c_1 = v_0, \quad (9)$$

$$\ddot{z} = 2c_2 + 6c_3 t + \dots \quad (10)$$

Inserting these series in (5) yields

$$2c_2 + 6c_3 t + 12c_4 t^2 + 20c_5 t^3 + \dots = g_0 + \gamma(c_0 + c_1 t + c_2 t^2 + c_3 t^3 + \dots). \quad (11)$$

Comparing the coefficients on the left side of the equation with the right side, the constants are obtained as

$$c_2 = \frac{1}{2}g_0 + \frac{1}{2}z_0\gamma, \quad c_3 = \frac{1}{6}\gamma v_0, \quad c_4 = \frac{1}{24}\gamma g_0 + \frac{1}{24}\gamma^2 z_0, \quad \dots \quad (12)$$

Considering the terms up to the order t^4 , (8) can be re-written as

$$z(t) = z_0 \left(1 + \frac{1}{2}\gamma t^2 + \frac{1}{24}\gamma t^4 \right) + v_0 \left(t + \frac{1}{6}\gamma t^3 \right) + \frac{1}{2}g_0 \left(t^2 + \frac{1}{12}\gamma t^4 \right). \quad (13)$$

Equation (13) is the observation equation which is used in absolute gravimetry to derive a g -value from the multiple time–distance measurement pairs in a least-squares adjustment. Because of its subtle contribution, the t^4 term in the z_0 -dependent expression can be neglected. The finite velocity of light c must be taken into account by adding the term z/c to the observed (raw) time values t' before the least-squares adjustment is carried out:

$$t = t' + \frac{z}{c}. \quad (14)$$

The reference height (position $z = 0$) of the derived free-fall acceleration g_0 depends on the setup of the instrument and should be defined by the operators with an accuracy of ± 1 mm to preserve the accuracy of the measurement system. For further theoretical considerations about the equation of motion in absolute gravimetry, it is recommended to study, e.g. Cook (1965) and Nagorny (1995).

In Torge (1993), a simple formula is given to assess the required accuracy for the time and distance measurements:

$$\frac{dg}{g} = \frac{dz}{z} - 2\frac{dt}{t}. \quad (15)$$

Equation (15) is obtained by the differentiation of (4) and setting z_0 and v_0 to zero. Asking for a relative accuracy $dg/g = 10^{-9}$ ($\equiv dg = 1 \mu\text{Gal}$) and considering a falling path of 0.2 m with a falling time of about 0.2 s, the accuracy requirement for the time and distance measurements is 0.2 nm and 0.1 ns, respectively. For state-of-the-art absolute gravimeters, this accuracy level is provided by the simultaneously performed atomic time and laser interferometric distance measurements.

1.3.3 Operational Procedures with FG5-220

Within the operational procedures with FG5-220, as employed at IfE, the time interval between two drops is 10 s which includes the reset of the falling corner cube and the online adjustment. For the reduction of local noise and other disturbances, 1,500–3,000 computer-controlled drops are performed per station determination. Generally, the measurements are subdivided into sets of 50 drops each and distributed over 1–3 days. The result of a station determination is the average of all

drops, reduced for gravity changes due to Earth’s body and ocean tides, polar motion and atmospheric mass movements, as explained in Sect. 1.5.

Relative gravimetric measurements are still highly important to transfer the absolute gravimetry results to network points at floor level or to another height level along the vertical that has been agreed on, e.g. for comparisons of different absolute gravity determinations. However, to preserve the accuracy of the absolute measurements for present and future investigations and applications, the absolute gravity result should not be affected by uncertainties in the vertical gradient due to measurement errors from relative gravimetry or deteriorated by unknown non-linearities in the gradient (Timmen 2003). These demands are fulfilled by defining the reference height close to a position where the influence of an uncertainty in the vertical gravity gradient becomes almost zero (“dead-gradient-point”); see Fig. 1.4. The corresponding position is approximately one-third of the falling distance below the first measured position of the free-fall trajectory as used in the adjustment computation (FG5-220: ~1.21 m above floor level). Therefore, all gravity determinations with the current Hannover FG5 instrument are referred not only to the ground floor mark but also to the reference height of 1.200 m above floor level or above the ground mark.

For the reduction of the absolute gravity value to the floor mark, the observed gravity difference (hereafter called gradient) is needed. Following the IfE standard procedure, the vertical gravity gradient is determined with two LaCoste and Romberg gravimeters with integrated feedback systems (Schnüll et al. 1984) or with a Scintrex Autograv CG3M (since 2002) using a tripod of about 1m height. By observing the difference 10 times with each relative meter, the gravity

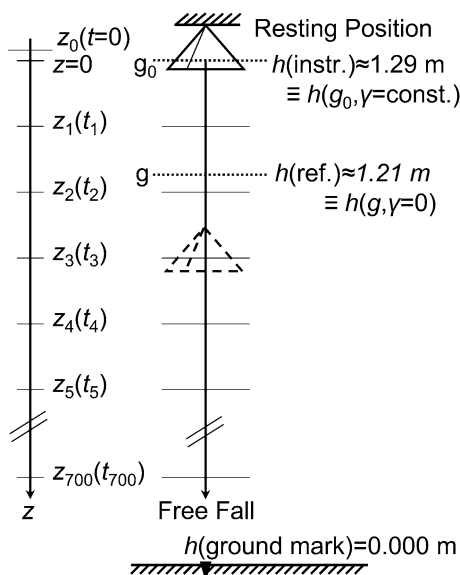


Fig. 1.4 Depending on the setup, the instrumental height of FG5-220 is around 1.29 m (top-of-the-drop). For geodynamic research, the g -value is referred to the fixed height 1.200 m above measuring mark to avoid uncertainties from the gradient assumption

difference is normally obtained with a standard deviation of about $1 \mu\text{Gal}$. Referring the gravity difference to a height difference of 1.000 m, the vertical gravity gradient γ is obtained. Here, a linear gravity change with height is assumed (constant gradient). For geodynamic research, often a more accurate knowledge about the vertical gravity change is required by considering a second-degree polynomial for the height dependency. In those cases, gravity differences Δg are measured between variable height levels h above the ground mark (cf. Fig. 1.5). A least-squares adjustment of observation equations provides an overconstrained solution for the coefficients γ_1 and γ_2 describing the linear and quadratic part of the polynomial:

$$\Delta g(h_i, h_j) = \gamma_1(h_j - h_i) + \gamma_2(h_j^2 - h_i^2). \quad (16)$$

With (16), an observed absolute gravity value with its defined reference height can be referred to any position within the perpendicular above the ground mark up to about 1.5 m (highest relative gravity measurement position).

For the site selection, preferences are given to buildings with a stable environment inside the observation room (stable temperature, no direct sun, relative humidity below 70%) and a solid foundation like a concrete pier, a reinforced concrete base slab or a concrete slab attached to bedrock.



Fig. 1.5 Measurement of the non-linear vertical gravity change along the perpendicular with a Scintrex relative gravimeter. Tripods are used for variable setup heights

1.3.4 Accuracy and Instrumental Offset

The manufacturers of the JILAg and of the FG5 systems performed an error budget analysis to determine the single instrumental uncertainty contributions through calculations and measurements of known physical effects. Niebauer (1987) derived a total error of $3 \mu\text{Gal}$ for JILAg instruments. In Niebauer et al. (1995) a total uncertainty of $1.1 \mu\text{Gal}$ is obtained from the FG5 instrumental error budget (Table 1.1).

To assess the accuracy of the transportable absolute gravimeters from the user point of view, the experiences with the Hannover instruments JILAg-3 and FG5-220 are used to derive an empirical accuracy estimate. For both instruments, the accuracy and stability have been continuously controlled by comparisons with other absolute gravity meters and with repeated measurements in several stations after time intervals of some months to a few years. A rigorous control of the absolute accuracy with respect to a “true” gravity value at the moment of an absolute gravity measurement is not possible. The real g -value with a superior accuracy is not known, and a “standard” absolute gravimeter which is superior to the state-of-the-art FG5 meters does not exist. Therefore, the empirical accuracy estimates have to

Table 1.1 Instrumental error budget of FG5 gravimeter and gravitational “noise” due to incomplete modelling and reduction of gravity variations with time, after Niebauer et al. (1995)

FG5 error source	Uncertainty [μGal]
Residual air pressure	0.1
Different temperature	0.1
Magnetic field gradient	0.1
Electrostatics	0.1
Attraction of apparatus	0.1
Verticality	0.1
Air-gap modulation	0.6
Laser wavelength	0.1
Corner-cube rotation	0.3
Coriolis effect	0.4
Floor recoil and tilt	0.1
Electronic phase shift	0.6
Frequency standard	0.2
Glass wedges	0.3
Diffraction limit	0.2
Total uncertainty (r.m.s.)	1.1
Gravitational “noise”	
Solid Earth tides	0.2–0.5
Equilibrium ocean load	0.2
Tidal swell and surge	5
Atmospheric attraction and loading	1–5
Groundwater table variations	Site-dependent
Polar motion	0.01
Microseisms (<100 Hz)	0

be understood as describing the agreement of the instruments' measuring level and their time stability with regard to the international absolute gravity datum definition. Here, the international datum is defined by the physical standards (time and length) and, in addition, as the average result obtained from all operational absolute gravimeters participating in the international comparison campaigns.

For JILAg-3, Torge (1991) estimated the short-term and long-term accuracy of a station determination between 5 and 10 μGal . On average, an accuracy estimate of 7 μGal was obtained. The instrumental precision by itself is assumed to be 4–5 μGal , which does not consider errors introduced by real gravity changes, e.g. due to subsurface water variation. For FG5-220, a realistic mean accuracy estimate seems to be about 3 μGal (cf. Timmen et al. 2006b; Francis and van Dam 2006; Francis et al. 2010; Bilker-Koivula et al. 2008). These empirical estimates incorporate

- Instrumental errors, e.g. due to instrumental vibrations or laser instabilities
- Gravitational “noise” due to incomplete modelling and reduction of gravity variations with time

Because most of the IfE measurements serve for local and regional gravimetric control, especially for geodynamic investigations in tectonically active areas, the long-term measuring stability of the two gravimeters is a major concern. To compare the results of JILAg-3 with recent observations of FG5-220, no systematic difference due to the gravimeters themselves should exist, or the instrumental offset should be well known. Within this context the instrumental offset should be understood as a mean measuring offset (bias) valid for a long time period, e.g. some years or even the gravimeters' lifetime. One possibility for detecting such an offset is to compare observation series of both instruments performed at a reference station where long-term stable gravity acceleration can be assumed (no significant secular change). The JILAg-3 reference station Clausthal in the Harz Mountains (stable bedrock) was occupied by FG5-220 at four different epochs in 2003 (January, May, June and October) to derive a reliable mean g -value for 2003 which is only slightly affected by seasonal hydrological changes. In Table 1.2, the mean result is compared with the mean from 29 gravity determinations with JILAg-3 performed in the

Table 1.2 Mean gravity values for station Clausthal (Germany) derived with JILAg-3 ($n = 29$ occupations, 1986–2000) and FG5-220 ($n = 4$ in 2003). The given s_i are standard deviations for a single gravity determination

JILAg-3/FG5-220 comparison	Remarks	Gravimeter	Period	Mean g -result [μGal]
Clausthal (Harz mountains)	IfE reference station for JILAg-3,	JILAg-3	1986–2000	981,115,734.5 $s_i = 4.9, n = 29$
	reference height 0.000 m	FG5-220	January–October 2003	981,115,725.1 $s_i = 2.3, n = 4$ $\Delta g = +9.4$

Table 1.3 Gravity differences (JILAg-3 minus FG5-101) obtained from the International Comparisons of Absolute Gravimeters (ICAG) in Sèvres 1994 and 1997 and during the surveying of the national German base network DSGN94 (five identical stations) and from three comparisons at the Clausthal reference station, after Torge et al. (1999)

Comparisons of JILAg-3 (IfE) and FG5-101 (BKG)	Discrepancy [μGal]
ICAG94, BIPM, pier A0	+9.0
ICAG97, BIPM, pier A	+8.1
DSGN94	+8.2
Clausthal reference station	+9.4

period 1986–2000. The standard deviation of the mean values is in both cases about $1 \mu\text{Gal}$. An obtained discrepancy of $+9.4 \mu\text{Gal}$ indicates a significant offset between the measuring levels of these two absolute gravimeters. Similar discrepancies have also been reported by Torge et al. (1999) when comparing measurements from FG5-101 (BKG) and JILAg-3 performed in the years 1994–1997. These comparisons showed a discrepancy varying between $+8.1$ and $+9.4 \mu\text{Gal}$ (Table 1.3). Figure 1.6 shows the time series of absolute gravity determinations at station Clausthal (point 522) observed with the two Hannover instruments (offset correction applied). The decline in the four observed g -values at the Clausthal station in 2003 should be connected to the very dry season in northern Germany. A similar but much stronger gravity change was measured in Hannover when the groundwater table fell 70 cm accompanied by a gravity decrease of about $13 \mu\text{Gal}$, see also Sect. 1.6.1.

By taking the offset correction of $-9 \mu\text{Gal}$ into account for all JILAg-3 observations, a stable measurement level for a time span of more than 20 years is assumed to be available with the two Hannover instruments. This is in accordance with the present knowledge that the FG5 series is presently the best instrumental realisation of absolute gravimeters. Nevertheless, to meet the accuracy requirements for long-term research over many decades and for comparability with other instruments, the observation level of the JILAg-3–FG5-220 couple has to be verified by comparisons with other absolute gravimeters. Since the 1980s,

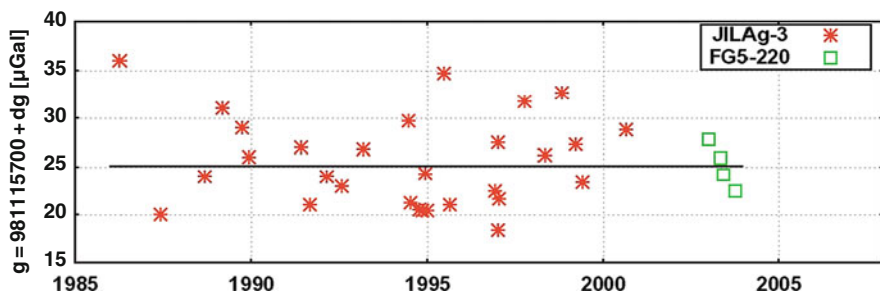


Fig. 1.6 Absolute gravity determinations with JILAg-3 and FG5-220 at station Clausthal (CLA522, trend $-0.1 \pm 0.2 \mu\text{Gal}/\text{year}$). An instrumental offset of $-9 \mu\text{Gal}$ ($\pm 1 \mu\text{Gal}$) was applied to the JILAg-3 results

International Comparisons of Absolute Gravimeters (ICAG) are performed at the Bureau International des Poids et Mésures (BIPM) in Sèvres and since 2003, with a 4-year time interval, also at the European Centre of Geodynamics and Seismology (ECGS) in Walferdange, Luxembourg. Such extensive comparison campaigns with a large number of absolute gravimeters may reveal biases not only between single instruments but also between different instrumental developments and technological realisations. Table 1.4 summarises the results from the comparisons ICAG89 (Boulangier et al. 1991), ICAG94 (Marson et al. 1995) and ICAG97 (Robertsson et al. 2001). In 1989, five JILA-type instruments and five individual developments participated. The JILAg-3 result differed from the mean of the JILA group by $+1.8 \mu\text{Gal}$, from the mean of the group with individual developments by $+3.3 \mu\text{Gal}$ and in the average by $+2.4 \mu\text{Gal}$ from the mean of all 19 stations' determinations performed by the 10 instruments. In 1994, for the first time FG5 instruments contributed to the comparison, and the discrepancy of JILAg-3 to the mean result of all 11 meters was $+2.8 \mu\text{Gal}$. These two comparisons may indicate a small offset of about $+2$ or $3 \mu\text{Gal}$ for JILAg-3. In 1997, the situations changed somewhat. The sites A and A2 were observed, and for both points the JILAg-3 result was $+5.5 \mu\text{Gal}$ above the average of all instruments. In addition to these external comparisons with other gravimeters, the lower part of Table 1.4 shows an internal comparison for JILAg-3. Looking at the Clausthal series with respect to the whole time span (1986–2000), and the two periods 1986–1996 and 1997–2000, a systematic change in the measuring level cannot be detected. The Clausthal series neither confirms nor contradicts the ICAG97 experience. Both results are consistent considering the precision estimate of $4\text{--}5 \mu\text{Gal}$ for a single station determination with JILAg-3.

From Table 1.4, it may be concluded that JILAg-3 was well embedded in the international absolute gravity definition. Overall, a larger discrepancy with other instrument groups did not really become obvious during the international comparisons. But a bias to the international standard, here defined as the average of all participating gravimeters at BIPM, of up to $+5 \mu\text{Gal}$ cannot be excluded. From the ICAG94 and ICAG97 comparisons, a measurement offset of $+9 \mu\text{Gal}$ becomes visible when just comparing JILAg-3 with FG5-101 as already mentioned. Thus, from the Hannover point of view, the offset correction for JILAg-3 has mainly to be considered as a bias with respect to the gravimeters FG5-220 and FG5-101 and not to the international standard. Interpreting the results of the international comparisons in Sèvres with respect to the instrument groups, a systematic error, inherent in the instrumental design of the JILAg or FG5 gravimeters, does not exist or is within the $1\text{--}2 \mu\text{Gal}$ accuracy level. Nevertheless, temporary biases for single instruments are possible, e.g. due to undetected changes within the instrumental adjustments.

To investigate the stability of the presently employed gravimeter FG5-220 of IFE, Table 1.5 gives the results from the international comparisons in Walferdange (Luxembourg) 2003 and 2007 (external comparisons, Francis and van Dam 2006; Francis et al. 2010) and FG5-220 reference measurements in Bad Homburg (station of BKG, Wilmes and Falk 2006) from 2003 to 2008. Within $2 \mu\text{Gal}$, the Hannover FG5 instrument agrees with the internationally realised measuring level. With respect to the FG5-220 observations in Bad Homburg, it has to be mentioned

Table 1.4 JILAg-3 absolute gravity meter controlled by external (international) and internal (repetition) comparisons to ensure consistent long-term measurement accuracy (n : number of observations)

JILAg-3 external comparisons	Remarks	Gravimeter group	Mean g result [μ Gal]	Standard deviation of a single observation [μ Gal]	Δg [μ Gal] (JILAg-3 minus mean)
ICAG89, BIPM (Boulanger et al. 1991, Table 7)	Referred to <i>site A</i> , reference height 0.050 m, 19 stations' determinations with 10 absolute gravimeters	5 JILAg-3 GABL, BIPM, IMGC, NIM, NAO	980,925,975.4 980,925,973.9	$\pm 6.2, n = 11$ $\pm 9.2, n = 8$	+1.8 +3.3
ICAG94, BIPM (Marson et al. 1995, Table 4)	Referred to <i>site A0</i> , reference height 0.900 m, 12 observations with 11 absolute gravimeters	All 10 meters Only JILAg-3 4 JILAg-3 6 FG5 1 IMGC	980,925,974.8 980,925,977.2 980,925,710.3 980,925,710.4 980,925,709.0	$\pm 7.4, n = 19$ $n = 2$ $\pm 4.9, n = 4$ $\pm 2.8, n = 7$ $n = 1$	+2.4 +2.7 +2.6 +4.0
ICAG97, BIPM (Robertsson et al. 2001, Table 5)	Occupied <i>site A</i> with 12 instruments, reference height 0.900 m	All 11 meters Only JILAg-3 4 JILAg-3 7 FG5 1 GABL-E	980,925,708.1 980,925,707.0 980,925,714.4 980,925,708.1	$\pm 3.3, n = 12$ $n = 1$ $\pm 5.5, n = 4$ $\pm 3.7, n = 7$ $n = 1$	+5.6 +6.6 -0.8 +5.5
ICAG97, BIPM (Robertsson et al. 2001, Table 5)	Occupied <i>site A2</i> with 13 instruments, reference height 0.900 m	All 12 meters Only JILAg-3 4 JILAg-3 6 FG5 IMGC, NIM-2a, ZZB	980,925,713.6 980,925,716.6 980,925,773.7 980,925,713.9	$n = 1$ $\pm 3.5, n = 4$ $\pm 2.9, n = 6$ $\pm 0.1, n = 3$	+3.5 +6.4 +6.2
		All 13 meters Only JILAg-3	980,925,714.6 980,925,720.1	$\pm 5.0, n = 13$ $n = 1$	+5.5

Table 1.4 (continued)

JILA-g-3 external comparisons	Remarks	Observation period	Mean <i>g</i> result [μ Gal]	Standard deviation of a single observation [μ Gal]	Δg [μ Gal]
Clausthal/Harz	IFE reference station for JILA-g-3, 29 observations over 15 years, floor level	Period 1986–2000 Only 1986–1996 Only 1997–2000	981,115,734.5 981,115,734.1 981,115,735.4	$\pm 4.7, n = 29$ $\pm 4.8, n = 20$ $\pm 4.6, n = 9$	-0.4 $+0.9$

Table 1.5 FG5-220 absolute gravimeter controlled by external (international) and internal (repetition) comparisons to ensure consistent long-term measurement accuracy

FG5-220 external comparison	Remarks	Epoch	Δg [μGal] (FG5-220 – mean g)
ICAG2003, ECGS (Francis and van Dam 2006, Table 16)	13 absolute meters, 14 points, 52 determinations	November 2003	–1.9 standard deviation (single instrument) 1.8
ICAG2007, ECGS (Francis et al. 2010, Table 3)	19 absolute meters, 16 points, 73 determinations	November 2007	+2.4 standard deviation (single instrument) 2.0
FG5-220 internal comparison	Remarks	Epoch	Δg (FG5-220) [μGal] (Single – mean g)
Bad Homburg (gravimetry lab of BKG, Wilmes and Falk 2006)	Reference station for FG5-220 since 2003, point BA	February 2003 November 2003 April 2005 April 2006 November 2007 September 2008	+0.9 –0.8 +1.2 +0.7 +0.2 –2.1

that the differences between the single epochs also contain real gravity changes due to time-varying environmental effects like seasonal hydrological variations. As shown in Table 1.5, the six stations' determinations agree very well, better than expected from empirical estimates, with a mean scatter of $1.1 \mu\text{Gal}$ only (root-mean-square difference, r.m.s.). An instrumental instability cannot be identified. A similar experience is also gained from the yearly repetition surveys and from the comparisons with the other FG5 absolute gravimeters involved in the Nordic absolute gravity project, to determine the Fennoscandian land uplift, cf. Timmen et al. (2006b) and Bilker-Koivula et al. (2008).

1.4 Relative Gravimetry

The determination of gravity differences and variations requires a composite employment of absolute and relative instrumental techniques and observation methods. The optimal choice of the different types of available sensors allows one to organise the work in a most efficient way with respect to accuracy and economy. Relative gravimetry contributes among others to the following geodetic tasks:

- Support of absolute gravimetry (centring to safety points, national net points or to adjacent absolute points; measurement of vertical and horizontal gradients)
- Monitoring of temporal gravity changes in investigation areas with short transportation time spans between the measuring points
- Densification of national gravity reference networks
- Providing dense point data to improve regional geoids

Fig. 1.7 Scintrex Autograv CG-3 (right) and CG-5 (left) and a LaCoste–Romberg model G with carrying case (in front)



The accuracies one strives for are in the order of one to a few tens of microgals. For high-precision relative gravimetry, LaCoste–Romberg (LCR) spring gravimeters have been employed nearly exclusively over decades. For about 20 years, Scintrex has offered a different type of spring gravimeter, the Autograv CG-3, e.g. see Hugill (1988), and since 2003 the new CG-5. Figure 1.7 shows a LCR and two Scintrex meters. Based on the inventions of L. LaCoste and A. Romberg, the company ZLS Corporation, Austin, TX, USA, designed the automated Burris Gravity Meter (ZLS 2007). The instrumental investigations described in Jentsch (2008) showed excellent results for the ZLS meter which may also be considered as a state-of-the-art instrument.

1.4.1 Principles of Spring Gravimeters

The principle of a vertical spring balance explains the general operation of a relative gravimeter. An elastic spring is used to generate a counterforce which keeps the sensor’s test mass in equilibrium with the gravitational force, see left part in Fig. 1.8.

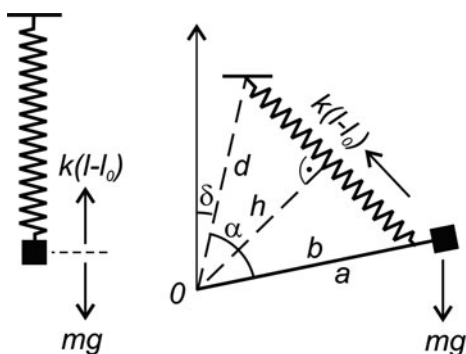


Fig. 1.8 The principle of a vertical spring balance (left) and of a lever spring balance (right)

For a translational system, which is in accordance with Hooke's law, the condition of equilibrium is given by

$$mg = k(l - l_0). \quad (17)$$

The spring constant k is the proportion of the stretching force, with mass m and gravity g , to the elongation ($l - l_0$) of the spring (l : spring length under load, l_0 : length without load). To determine a gravity difference Δg , the small change in the spring length Δl has to be measured:

$$\Delta g = \frac{k}{m} \Delta l. \quad (18)$$

For that, a reading system with an extremely high resolution is required. To achieve a measuring precision of better than $10 \mu\text{Gal}$, the mechanical sensitivity of about 0.1 nm is needed with a corresponding time stability of the spring force. A precise knowledge of the calibration factor k/m can nowadays be obtained by measurements between well-known absolute gravity points.

The right part of Fig. 1.8 shows the general lever spring balance. The equilibrium condition for the torques generated by gravitational force mg and spring force $k(l - l_0)$ can be expressed with

$$mga \sin(\alpha + \delta) = k(l - l_0)h = k(l - l_0)b \frac{d}{l} \sin \alpha. \quad (19)$$

The equation shows a non-linear relation between gravity g and angle α . With the conditions

$$l_0 = 0 \text{ ("zero-length spring")} \quad \text{and} \quad \alpha + \delta = 90^\circ, \quad (20)$$

(19) simplifies to

$$mga = kbd \sin \alpha. \quad (21)$$

Choosing the angles

$$\alpha \rightarrow 90^\circ \quad \text{and} \quad \delta \rightarrow 0^\circ \quad (22)$$

increases the mechanical sensitivity considerably ("astatisation").

The requirements in (20) and (22) are implemented in the design of LaCoste-Romberg gravimeters with a counterspring made of metal (Krieg 1981). To achieve a measuring precision of better than $10 \mu\text{Gal}$, a pick-off system with a resolution of a few hundred nanometers is needed only. Measurements with LCR meters require a very accurate alignment of the mass-beam part to the horizontal orientation. Due to a gravity change, the test mass diverges from the horizontal position which can be restored by turning a dial which moves the suspension point of the spring up or down (zero-method, "nulling" the beam). The whole transmission system consists of the

dial, a set of gear wheels, the measuring screw and a lever system. The difference between two readings of the dial, which is combined with a counter, corresponds to a gravity difference. In addition to this mechanical compensation for restoring the zero position, an electronic feedback system is used nowadays. The moveable middle part of a three-plate capacitor is attached to the test mass, which allows an electrical pick-off of the sensor position and a restoring to the zero position. The electronic feedback systems help to avoid periodical errors due to imperfections in the gear-screw construction (Schnüll et al. 1984; Röder et al. 1988).

With the technical advances in the 1980s, the company Scintrex, Concord, Ontario, Canada, was able to design a new relative gravimeter using the principle of the vertical spring balance. The Scintrex CG-3 and CG-5 gravimeters are non-astatised systems with a quartz spring which covers the worldwide gravity range and operates without any micrometer screw or gearbox. The capacitive transducer and electronic feedback system allows a pick-off resolution of 0.2 nm (Scintrex 1998). Besides the non-existence of periodic errors, an additional advantage of the linear spring system is that the sensitivity is independent of the inclination. The new Burris Gravity Meter from ZLS Corporation, which is based on the LCR astatisation principles with a lever spring balance, is equipped with a digital feedback system of about 50 mGal range to null the beam. The zero-length spring is made by a metal alloy and is characterised by its low drift (Jentzsch 2008).

For more details and a more extensive overview about the principles of relative gravimeters, refer to other available literature, e.g. Torge (1989).

1.4.2 Observation Equation

To transfer a raw gravimeter reading, here given in counter units, to a gravity value, the calibration has to be known. In addition, a time-dependent instability of the counterforce (fading of the spring tension) should be considered in the observation equation. Environmental disturbances, e.g. small temperature changes within the sensor case or mechanical impulses caused by transportation, may change the gravimeter's reading considerably. This instrumental drift can be modelled by a low-order polynomial and requires repeated measurements, temporally well distributed over the measuring period, of at least some of the network points. The following equation gives the connection between the raw reading and the resulting g -value for a LCR gravimeter:

$$g = N_0 + \sum_{j=1}^p d_j(t - t_0)^j + \sum_{k=1}^m Y_k z^k + \sum_{l=1}^n A_l \cos(\omega_l z - \phi_l), \quad (23)$$

with N_0 = instrument level, d_j = drift parameter of degree j , t_0 = starting time (e.g. first daily measurement), Y_k = calibration coefficient of degree k , z = reading in counter units, A_l = amplitude, ω_l = frequency, ϕ_l = phase of the periodic term of degree l . Often the so-called Δg adjustment of a gravity network is applied,

Table 1.6 Maximum and mean amplitude of the periodic calibration terms as derived for 21 LaCoste–Romberg model G gravimeters in the gravimeter calibration system Hannover

Periods	Up to LCR-G457	1.00	7.88	35.47	70.94
[CU]	From LCR-G458	1.00	7.33	36.67	70.33
Maximum amplitude		8.1	15.2	21.5	18.0
Mean amplitude in [μ Gal]		2.5	5.2	5.9	8.0

which introduces gravity differences between two successive point measurements. The advantage is the elimination of the unknown N_0 -parameter in the observation equation. For Scintrex CG meters, the periodic terms in (23) do not exist.

Table 1.6 summarises the magnitude of periodic errors for 21 LCR gravimeters as determined in the gravimeter calibration system Hannover. Neglecting these errors, an additional uncertainty (systematic error) of a few tens of microgals can be possible for gravity differences. Comparisons of the results for three LCR instruments from IfE, all three employed in the calibration systems Hannover and Wuhan/China (different gravity ranges), showed significant discrepancies for the polynomial and periodical calibration parameters (Xu et al. 1988). Therefore, for highly accurate measurements it is advised to examine the meter's calibration when transferring the parameters to different gravity ranges (recommendation from the author: for distances of more than 0.5 Gal away from the calibration system).

1.4.3 Regional and Local Surveys with Scintrex SC-4492

In 2001, IfE obtained the new Scintrex CG3 gravimeter no. 4492. The following investigations of this state-of-the-art relative gravimeter were focussed on the calibration (time stability and gravity range dependency). The study was performed over a time period of about 4 years and covered a gravity range of almost 1.5 Gal. In addition, other publications can be recommended to achieve a more general overview about the quality of the Scintrex Autograv CG-3 system, e.g. Hugill (1988), Jousset et al. (1995), Falk (1995), Rehren (1997) and Everaerts et al. (2002). With respect to instrumental precision, accuracy and drift, the IfE investigations confirm the results of the references given above.

Most of the surveys with the SG-4492 were carried out in the gravimeter calibration system Hannover; see Fig. 1.9. This was established between 1976 and 1982 for the determination of calibration functions for LCR gravimeters with 1μ Gal accuracy (Kangieser et al. 1983). The system serves for the analysis of polynomial and periodic calibration terms, with the intent of improving the manufacturer's calibration tables which usually provided accuracies of 10^{-3} to 10^{-4} only. Over 13,000 gravity differences measured with 47 LCR instruments and 12 absolute gravity determinations were included in the adjustment of the calibration system. The estimated mean standard deviations for the adjusted gravity differences are 2μ Gal for the Cuxhaven–Harz line (~ 9 mGal intervals) and 1μ Gal for the vertical calibration

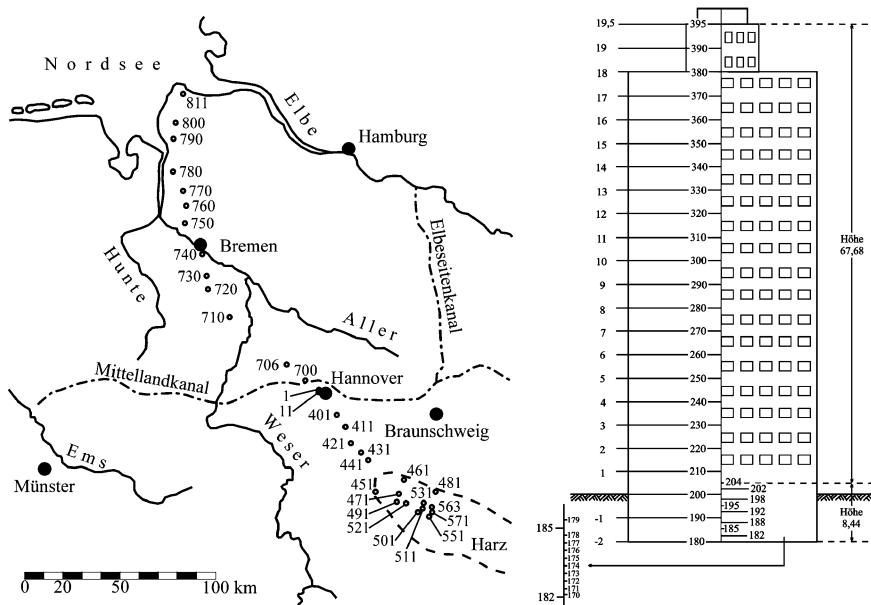


Fig. 1.9 The station distribution of the gravimeter calibration system Hannover (Cuxhaven–Harz Mountains, 300 mGal, and vertical calibration line Hannover, 20 mGal), cf. Torge (1989)

line Hannover (staircase of a 20-storied building, point intervals of 0.02, 0.2 and 1 mGal).

From November 2001 to September 2005, the SC-4492 has been employed in different projects in northern Germany and in Scandinavia; see Fig. 1.10. In most cases the instrument has been transported not only by hand but also by car. In general, the measurements were done using the step method to allow an optimal drift control, e.g. with a point sequence A-B-A-B-C-B-C-D-C-D. Each tie between neighbouring points was measured three times or more with a time span of 5–60 min between the two successive point occupations. Only during the absolute gravimetry campaigns in Fennoscandia in 2004 and 2005, the relative measurements between the absolute stations were observed once with a long time span of up to 10 h between the two successive readings. For each occupation three registrations with a read time (RT) of 60 s and a cycle time (CT) of 80 s were carried out. The seismic filter option of the online software was selected. The average of the second and third cycle was used for the post-processing with the program system GRAV from Wenzel (1993). The least-squares adjustment provides accuracy estimates for the single gravity difference observations in the order of 4–10 μ Gal when excluding the two long-distance campaigns in Fennoscandia. Measuring gravity ties with short transportation ways, points can be connected within an accuracy level of about 1 μ Gal. The points in the Harz Mountains (461–571) show small discrepancies between the calibration line reference values and the recent results from SC-4492. The differences vary between -3.8 and $+3.1$ μ Gal with an r.m.s. discrepancy of 2.4 μ Gal.

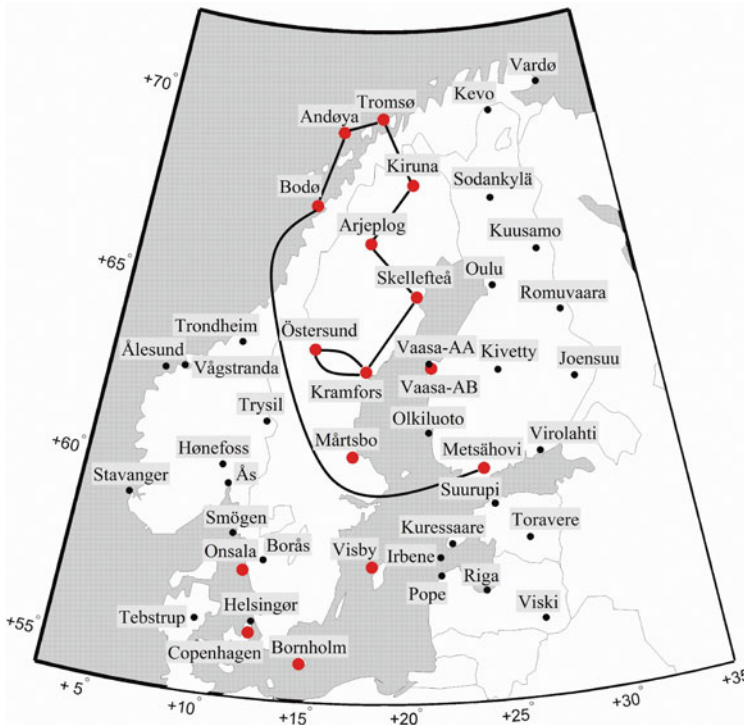


Fig. 1.10 Absolute gravity stations in the Fennoscandian land uplift area occupied by FG5-220 in 2004 (red dots). Lines show the ties used to control the calibration of the relative gravimeter SC-4492

For the northern part of the calibration line, the differences are much larger (maximum $+6.5 \mu\text{Gal}$ and minimum $-11.4 \mu\text{Gal}$, r.m.s. $6.8 \mu\text{Gal}$). Besides measurement errors, the large discrepancies can also be caused by groundwater and soil moisture effects and/or secular gravity changes during the last 20 years.

Table 1.7 summarises the calibration results obtained for SC-4492, standing as an example for a present-day advanced relative gravimeter. Polynomial calibration terms of higher degree were not found. The calibration factors E (improvement of the manufacturer calibration) were obtained with a precision between 2 and 8×10^{-5} and are varying within a range of 3×10^{-4} . Calculating a mean factor and expressing the single deviations from the mean in gravity discrepancies (last column), disagreements up to almost $20 \mu\text{Gal}$ were found. But these values cannot be assigned to instabilities or gravity range dependencies of the calibration factor. The uncertainties in the reference gravity values and, moreover, the subsurface water mass changes (groundwater, soil moisture, crevasses and clefts in rock filled with water) can introduce errors of more than $10 \mu\text{Gal}$. Therefore, a time-dependent instability of the calibration in the order of 1×10^{-4} cannot be excluded but is also not proven. In addition, the calibration results show no correlation with the different

Table 1.7 Calibration of Scintrex CG-3 no. 4492 in different gravity ranges over 4 years (adjustment results: calibration factor, accuracy, drift), total gravity range: 1,468 mGal

Project	Date	Δg (max) [mGal]	n	Δg	E	Drift [μ Gal/h]	s (Δg) [μ Gal]	ΔE [$\times 10^{-6}$]	$\Delta E \rightarrow \delta g$ [μ Gal]
Calibration line Hannover-Cuxhaven	23.11.2001	118	4		1.000854 \pm 0.000026	18.7	± 13.5	65	+7.7
Connection of two absolute stations Hannover-Harz	04.07.2002	147	4		1.000912 \pm 0.000034	24.8	± 10.2	7	+1.0
Calibration line Hannover-Harz	05.11.2002– 22.01.2003	190	104		1.001011 \pm 0.000025	18.0	± 10.5	-92	-17.5
Connection of two absolute stations Hannover-Harz with intermediate points	14.11.2002– 28.11.2002	147	42		1.001031 \pm 0.000031	16.9	± 5.4	-112	-16.5
Calibration line Hannover-Cuxhaven	23.01.2003– 15.02.2003	117	127		1.001062 \pm 0.000060	11.7	± 9.9	-143	-16.7
Connection of two absolute stations Hannover-Hamburg	27.02.2003	108	13		1.000786 \pm 0.000020	19.6	± 3.7	133	+14.4
Calibration line Harz mountains	21.04.2004	93	14		1.000872 \pm 0.000026	32.7	± 8.1	47	+4.4
Fennoscandian land uplift area 2004	02.06.2004– 02.07.2004	623	16		1.000945 \pm 0.000076	13.0	± 24.7	-26	-16.2
Calibration line Harz mountains	13.04.2005	93	11		1.000836 \pm 0.000027	9.8	± 7.4	83	+7.7
Fennoscandian land uplift area 2005	20.08.2005– 25.09.2005	445	12		1.000878 \pm 0.000042	11.4	± 23.6	41	+18.3
Mean					1.000919 \pm 0.000029	17.7 ($\equiv 0.43$ mGal/day)			

n Δg : number of Δg measurements; E : adjusted linear calibration factor; drift: adjusted linear drift factor; s (Δg): standard deviation of a single Δg measurement; ΔE : deviation from mean E ; $\delta g = \Delta E \times \Delta g$ (max)

gravity ranges which lead to the conclusion that no gravity range dependence exists over the total investigation range of 1,470 mGal.

1.4.4 Microgravimetric Measurements

Highest accuracy can be expected for measurements in a small network with points distributed in one room or in a single building (short time spans between measurements, meter transportation manually (shock prevention), no wind, stable temperature). In an extensive survey, the vertical calibration line in Hannover has been measured with SC-4492 (31 points, 328 gravity difference observations), cf. Table 1.8. The standard deviation for a single gravity difference measurement is just 3.7 μ Gal. Figure 1.11 reveals a systematic discrepancy between the calibration line reference values and the new determined figures. The differences for the points above ground floor show a height and gravity dependence which can be interpreted as a linear scale error of about 3×10^{-4} ($\equiv 6.0 \mu$ Gal). After these investigations with SC-4492, it cannot be excluded that the vertical calibration line is deteriorated by a small-scale error. Additional investigations with another CG-3 or CG-5 are needed to clarify this issue. One reason for the discrepancies of points below ground floor may be due to the different gravimeter setups. The LCR meter has normally an average sensor height of about 6 cm above floor level. The CG-3 system with its tripod measures the gravity at a height of about 27 cm. The points are all in corners very close to the walls, only 20 cm away. The not well-known gravity gradients along the vertical, with their non-constant behaviour, disturb the comparison of the different gravimeter systems. The r.m.s. discrepancy between the recent SC-4492 results and the reference values is 2.3 μ Gal.

The determination of vertical gravity gradients is important, because the combination of instruments with different reference heights strongly needs a highly precise centring of the measured gravity values to a common reference. Vertical gradients were observed at the two absolute gravity stations of IfE, Hannover and Clausthal, and at stations of the Fennoscandian uplift area, cf. Tables 1.8 and 1.9. With the help of a tripod of 1 m height, the gravity difference is measured to determine the gradient, cf. Fig. 1.5. Because of the sensor height difference between the LCR and the CG-3 systems (about 21 cm), the results from the two kinds of meters can differ by some 1 μ Gal. The LCR meters of IfE are equipped with the SRW-feedback systems, which eliminates the problems with periodic errors and gravity dependencies for small gravity differences (Röder et al. 1985). Figure 1.12 shows the absolute gravity meter setup on the pier in the basement of station Clausthal. A mesh of nine points with a spacing of 40 cm has been surveyed with SC-4492 to determine the horizontal gravity field above the pier surface. The result (Fig. 1.12, right) seems to be reasonable. With distance to the wall (cf. Fig. 1.12, left), gravity increases by about 2.5 μ Gal per 10 cm.

The obtained accuracies for all microgravimetric surveys are in the order of 1–2 μ Gal. In Table 1.9, three vertical gradients are compared with LCR results. In all cases the obtained results from SC-4492 are smaller than the LCR results which

Table 1.8 Network and adjustment statistics/results (accuracy, drift, etc.): re-measurements of 31 points of the vertical calibration line Hannover, determination of gravity gradients with Scintrex CG-3 no. 4492

Project (indoor observations)	Date	Δg (max) [mGal]	Number of points	$n \Delta g$	Δt [min]	Drift [μ Gal/h]	s (Δg) [μ Gal]	s (point) [μ Gal]
Vertical gravity calibration line Hannover	18.05.2002– 6.08.2002	19.2	31	328	~7–10	25.1	± 3.7	± 1.2
Vertical gravity gradient at absolute station Hannover	05.12.2002	0.30	2	20	~5–6	7.4	± 2.4	± 0.5
Vertical gravity gradient at absolute station Clausthal/Harz	30.01.2003	0.27	2	20	~3	0.4	± 4.2	± 0.9
Horizontal gravity gradient at absolute station Clausthal	30.01.2003	0.02	9	47	~3	4.7	± 4.6	± 1.4
Eleven vertical gravity gradients in the Fennoscandia uplift area	August/September 2003	0.38	11 \times 2	11 \times 10	~5–6			± 1.7

$n \Delta g$: number of Δg measurements; Δt : time span between successive observations; drift: adjusted linear drift factor; s (Δg): standard deviation of a single Δg measurement; s (point): standard deviation (mean) for a gravity point.

Fig. 1.11 Differences between the reference values of the vertical calibration line and the new determined gravity values with SC-4492

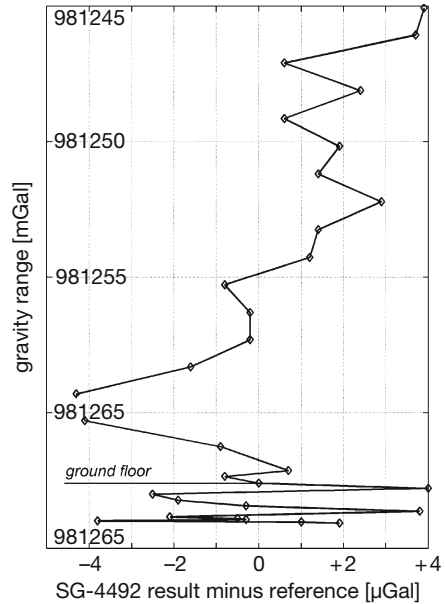


Table 1.9 Comparison of the SC-4492 results with reference results (all determined with LCR gravimeters)

Project	Comparative figures	Difference to SC-4492
Vertical gravity calibration line Hannover	Calibration line reference values	$\pm 2.3 \mu\text{Gal}$ (r.m.s.)
Vertical gravity gradient at absolute station Hannover	Five LCR SRW-feedback meters in 1993/1994, mean: $303.1 \mu\text{Gal/m}$	$+1.8 \mu\text{Gal/m}$
Vertical gravity gradient at absolute station Clausthal/Harz	Four LCR SRW-feedback gravimeters in 1987, mean: $266.0 \mu\text{Gal/m}$	$+3.0 \mu\text{Gal/m}$
Vertical gravity gradient at absolute station Vaasa (AB)	Simultaneous observation with LCR-G709 SRW-feedback gravimeter in 2003: $330.7 \mu\text{Gal/m}$	$+2.8 \mu\text{Gal/m}$

are reasonable for these stations considering the different sensor heights above the massive concrete piers.

1.4.5 Instrumental Drift

The gravimeter drift can be differentiated into two parts: stationary drift mainly due to spring aging and the transportation drift which may be caused by small shocks, vibrations, temperature effects or hysteresis effects after sudden changes of

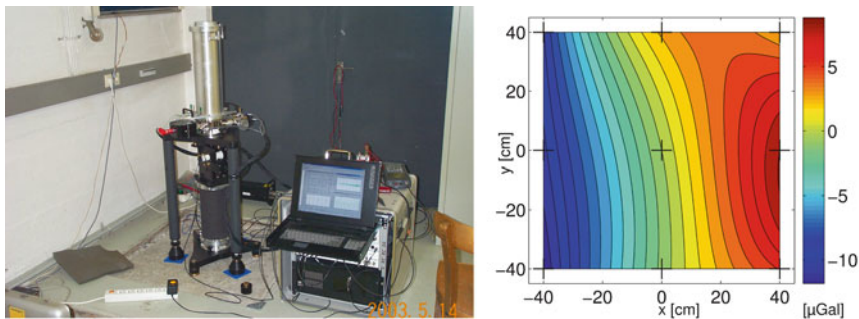


Fig. 1.12 The FG5-220 occupying the absolute gravity point at station Clausthal; contour plot of the horizontal gradient field above the pier with 1 μGal intervals

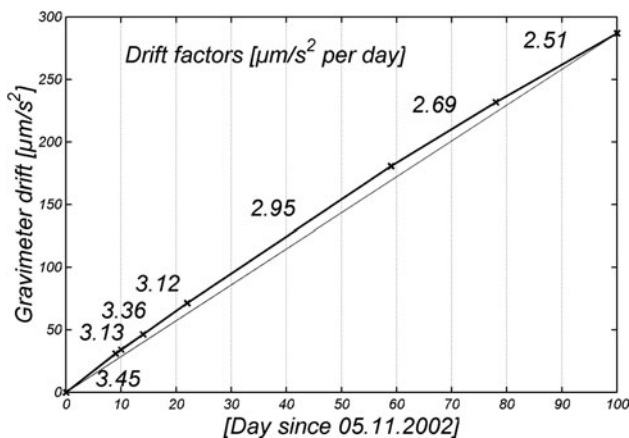


Fig. 1.13 Long-term drift (composition of stationary and transport drift) of SC-4492

the spring load (e.g. mechanical unclamping of the lever). A long-term drift (composition of stationary and transportation drift) of the meter is shown in Fig. 1.13. On 8 different days within a time span of 100 days, the first reading in the morning on a common starting point has been used to derive this long-term behaviour. The figure depicts a nearly linear behaviour.

Table 1.10 summarises the adjusted linear drift factors from daily field surveys obtained on 14 different days. It becomes clear that the drift behaviour of SC-4492 during the field surveys is significantly not linear. The drift can vary enormously. Therefore, for precise geodetic measurements a drift behaviour has to be taken into account as a non-linear temporal change of the zero level of the gravimeter’s readings. The drift is determined by repeated point occupations during a day which allows a modelling by a low-order polynomial with time; see (23). Depending on the network structure, the instrumental behaviour and the required accuracy, different measurement methods can be applied to control and determine the drift of

Table 1.10 Adjusted linear daily drift factors from daily field surveys with SC-4492

Date	Number of points	Number of Δg observations	Measuring time [h]	Drift [$\mu\text{Gal}/\text{d}$]
05.11.02	11	14	8	436
14.11.02	5	12	9	361
15.11.02	7	19	6	532
20.11.02	2	10	2	433
28.11.02	3	10	6	383
05.12.02	2	20	2	177
04.01.03	2	9	5	309
21.01.03	4	6	4	378
22.01.03	2	4	2	592
23.01.03	4	5	6	69
05.02.03	3	6	6.5	78
12.02.03	4	9	6.5	-49
15.02.03	2	10	3	412
27.02.03	2	3	6.5	469
			Mean	327 ± 189

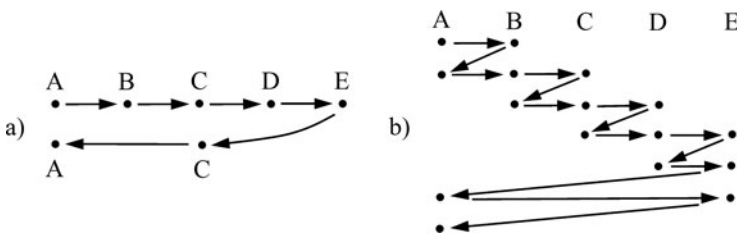


Fig. 1.14 Measuring procedures for drift control: (a) profile method with weak drift control, (b) step method with strong drift control (three times each tie and overlaps)

an instrument which is shown in Fig. 1.14. In general, the step method is used for most precise surveys. For example, the Hannover gravimetry group applies the five times step method to calibrate gravimeters with electronic feedback systems using the vertical calibration line in the 20-storied university building.

1.5 Reduction of Non-tectonic Gravity Variations

The Earth’s gravity field varies continuously with time which is explained in detail, e.g. by Torge (1989). For geodynamics research, the establishment of regional gravity control networks and the establishment of globally distribute absolute gravity stations serve to reveal gravity changes of long-term or secular character. Such changes may occur together with tectonic plate movements, with postglacial isostatic compensation processes, with tectonic processes like mountain building or with compactions in sediment basins. Local gravity changes of short-term or even

abrupt character may become detected by gravity monitoring nets covering areas with volcanism or earthquakes. In addition, human activities can cause significant variations in the Earth’s gravity field (large constructions, withdrawal of water, oil, gas, etc.). All gravimetric measurements are subject to irregular and periodic changes caused by tides, groundwater and other hydrological processes (e.g. soil moisture variations), atmospheric mass movements and polar motion. These effects of non-tectonic causes are superimposed on the target signal and have to be removed as well as possible. Generally, gravimetric measurements are freed from effects of the tides, the atmospheric mass redistributions and the small movements of the Earth’s rotation axis within the Earth. The transfer function between changes in the groundwater table and the related gravity effect at the measurement point is often not well known, and therefore the latter is not a standard reduction in gravimetry. Torge et al. (1987) describe the reductions for absolute gravity measurements with the Hannover JILA absolute meter.

1.5.1 Earth’s Body and Ocean Tides

The tidal deformation of the Earth is an elastic response of its body to the gravitational accelerations produced by the Moon, the Sun and, to a slight extent, also by the planets (Wang 1997; Wenzel 1997). At mid-latitudes periodical deformations over a day occur with an amplitude range of up to 40 cm. The maximal gravity variation remains below $300 \mu\text{Gal}$. The solar tides amount to 46% of the lunar tides.

In the Earth’s centre of mass, the gravitation of the other celestial bodies is completely compensated by the centrifugal accelerations due to the orbital motion of the Earth. Figure 1.15 shows a simplified version of the Earth–Moon system with a non-rotating Earth and the Moon as a point mass. The motion of the Earth around the barycentre of the two-body system generates the orbital acceleration $-b_0$ which is a constant for all points within the body and on the surface of the Earth. Because of the spatial extension of the Earth, the gravitation vector b differs from position to position. The tidal acceleration b_t for point P on the Earth’s surface is the sum of the gravitation b and the orbit acceleration $-b_0$. Applying Newton’s gravitational law, the tidal acceleration vector for the Moon is given by

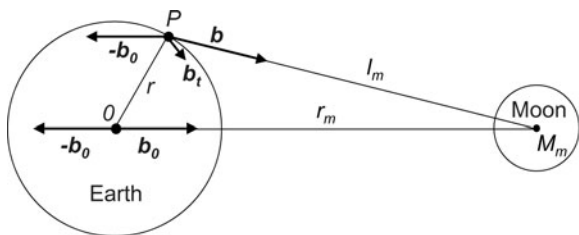


Fig. 1.15 Tidal acceleration as the sum of the Earth’s orbital acceleration and lunar gravitation

$$b_t = b - b_0 = \frac{GM_m}{l_m^2} \frac{\mathbf{l}_m}{l_m} - \frac{GM_m}{r_m^2} \frac{\mathbf{r}_m}{r_m}, \quad (24)$$

where M_m is the mass of the Moon, G the gravitational constant, l_m and r_m the distances between point P and the Moon and between the Earth's centre of gravity O and the Moon, respectively.

Because of the Earth's rotation and the continuously varying distances of the Sun and the Moon from the Earth, a large number of waves (partial tides) have to be considered to model the theoretical tides for a rigid (not deformable) Earth's body. The ephemerides of the celestial bodies are well known from astronomy which allows the precise calculation of the rigid Earth tides. The tidal spectrum comprises a long-periodic part with half-monthly, monthly, semi-annual, annual and longer periods and short-periodic waves with the main power in the daily and half-daily periods. The longest wave with 20,942 years is the period of the mean ecliptic longitude of the sun's perigee. The widely available harmonic developments of the tidal potential follow the spectral representation as chosen by Doodson (1921). In the more recent literature, a detailed mathematical description can be found, among others, in Wenzel (1997). Tidal potential catalogues with different accuracies contain up to more than 1,000 waves. The most common catalogues are from Cartwright, Taylor and Edden (Cartwright and Taylor 1971; Cartwright and Edden 1973) with 505 partial tides (accuracy better than $0.1 \mu\text{Gal}$) and from Tamura (1987) with 1,200 waves ($0.01 \mu\text{Gal}$). The model from Hartmann and Wenzel (1995) with 12,935 waves also includes coefficients due to the nearby planets and to the flattening of the Earth. An extensive description of the principal waves of the theoretical tides (rigid Earth) is given in Zürn and Wilhelm (1984).

Gravimetric Earth tide measurements show large differences with respect to the theoretical tides which can be explained by the non-rigid behaviour of the Earth's body and by effects from the ocean tides. The astronomical tide generating forces cause an elastic deformation of the solid Earth. Compared to the model of the rigid Earth, the amplitudes of the partial tides of the solid Earth are amplified and a phase shift takes place. In addition, the ocean tides affect the gravity measurements by the direct attraction of the moving water masses and indirectly by the resulting deformation of the crust due to the water load (ocean load tides). In general, close to the ocean the tidal loading effect is much smaller than the body tides but still affects gravity to very large distances from the coast (Jentzsch 1997). The ocean loading signal is not in phase with the body tides.

To reduce gravimetric measurements for Earth's body and ocean tides, the gravimetric tidal reduction as a compound tidal signal can be described as a sum of periodic terms:

$$\Delta g_{\text{tid}} = - \sum_{i=1}^n \delta_i A_i(\text{theor}) \cos(\omega_i t + \Phi_i(\text{theor}) + \Delta\Phi_i) \quad (25)$$

$$\text{with amplitude factor} \quad \delta_i = A_i \div A_i(\text{theor}) \quad (26)$$

Table 1.11 Principal gravimetric partial tides and the measured amplitude factors and phase leads (station Hannover: $\varphi = 52.389^\circ$, $\lambda = 9.714^\circ$). The Earth tide registrations with spring gravimeters in Hannover did not allow the evaluation of long-periodic tidal waves due to the instrumental drift behaviour. The partial tide with 18.6 years (6,798.4 days) has no special symbol

Tide symbol	Period [solar days/h]	Amplitude (theor) [μGal]	Amplitude factor δ []	Phase lead $\Delta\Phi$ [$^\circ$]
Constant lunar and solar tides				
M_0S_0	∞	26.7	–	–
Long-period tides				
–	6,798.4 days	2.4	–	–
Sa	365.26 days	0.4	–	–
Ssa	182.62 days	2.6	–	–
Mm	27.55 days	2.9	–	–
Mf	13.66 days	5.6	–	–
Diurnal tides				
Q_1	26.87 h	5.8	1.151	0.05
O_1	25.82 h	30.0	1.150	0.15
P_1	24.07 h	14.0	1.149	0.11
K_1	23.93 h	42.3	1.140	0.13
Semidiurnal tides				
N_2	12.66 h	5.4	1.176	2.34
M_2	12.42 h	28.0	1.186	1.68
S_2	12.00 h	13.0	1.189	0.41
K_2	11.97 h	3.5	1.191	1.07
Terdiurnal tides				
M_3	8.28 h	0.3	1.068	0.47

$$\text{and phase lead } \Delta\Phi_i = \Phi_i - \Phi_i(\text{theor}). \quad (27)$$

The frequencies of the partial tides $\omega_i = 2\pi/T_i$ (T : period), the amplitudes $A_i(\text{theor})$ and the phases $\Phi_i(\text{theor})$ are already derived from the models for the theoretical tides. The amplitude factor δ is also called gravimetric factor and can be determined together with the phase lead $\Delta\Phi$ by comparing the results of a continuously recording relative gravimeter with the rigid (theoretical) Earth tides. Table 1.11 summarises the results of Earth tide registrations in Hannover with five LCR gravimeters equipped with SRW-feedback systems (Timmen and Wenzel 1994). In the past, the global factor $\delta = 1.16$ was often used for all tidal waves in case of not existing observed parameters.

In contrast to tidal observations, the gravimetric tides can be computed on the basis of a model of the Earth's body determined from seismology, e.g. Preliminary Reference Earth Model (PREM) from Dziewonski and Anderson (1981), and using a global ocean model derived from satellite altimetry or from tide gauge observations as done by Schwiderski (1980). The latter used tidal observations of tide gauges along the continental coasts and on islands and developed a hydrographical interpolation model. For the first time, a global model was available describing the tidal response of the ocean's water masses. With the successful satellite altimetry

missions like Geosat (1985–1990), TOPEX/Poseidon (1992–2006) and some others, direct measurements of the ocean’s surface height were evaluated to provide accurate ocean tide models. Because Schwiderski’s model is still accurate enough, it is widely used for the tidal reduction in absolute and relative gravimetry.

At IfE in Hannover, the series development from Tamura (1987) delivers the tidal effects for the solid Earth, with synthetic tidal parameters (amplitude factors and phase shifts) interpolated from a worldwide $1^\circ \times 1^\circ$ grid (Timmen and Wenzel 1995) to take the Earth’s elastic behaviour into account. This grid was computed from

- Body tide amplitude factors using the Wahr–Dehant model (Wahr 1981; Dehant 1987) of an ocean-free, uniformly rotating and ellipsoidal Earth with inelastic mantle, liquid outer core and elastic inner core
- Ocean tide gravitation and load (Agnew 1997) derived from a $1^\circ \times 1^\circ$ ocean tide model (Schwiderski 1980)

For the time-constant M_0S_0 tides, the amplitude factor 1.000 and a zero phase shift are used according to the IAG standards (Rapp 1983, “zero-tidal gravity”). For absolute gravity measurements the uncertainties in the geographical coordinates should be less than 10" with a height accuracy of better than 100 m. The time of a gravity observation can easily be recorded with better than 10 s UTC. Because the measurements of a station determination are distributed over 1–3 days, the average result can only be affected by residual errors of some $0.1 \mu\text{Gal}$ (Timmen 1994). Near the coasts, larger uncertainties are possible.

1.5.2 Polar Motion

The Earth’s rotation vector varies its orientation with respect to the Earth’s crust. The penetration points of the rotation vector through the Earth’s surface, the poles, are subject to motions of several metres per year. Figure 1.16 depicts the winding curve of the instantaneous North Pole relative to the reference pole of the International Earth Rotation and Reference Systems Service (IERS). The plotted x_p and y_p pole coordinates are provided by IERS on their internet pages. They are defined in a plane tangential to the pole with the x -axis in the direction of the Greenwich mean meridian and the y -axis points to the 90°W meridian. The polar motion consists mainly of two periodic components and a long-term irregular drift (cf. Figs. 1.16 and 1.17):

- The Chandler period (wobble) of 435 days has an amplitude of about 0.1" to 0.2" (3–6 m). This free oscillation is due to the dynamical flattening of the Earth and is excited when the instantaneous rotations axis deviates from the principal axis of inertia (figure axis). The mass displacements in the atmosphere and in the oceans exert torques on the solid Earth and excite the Chandler wobble continuously. An

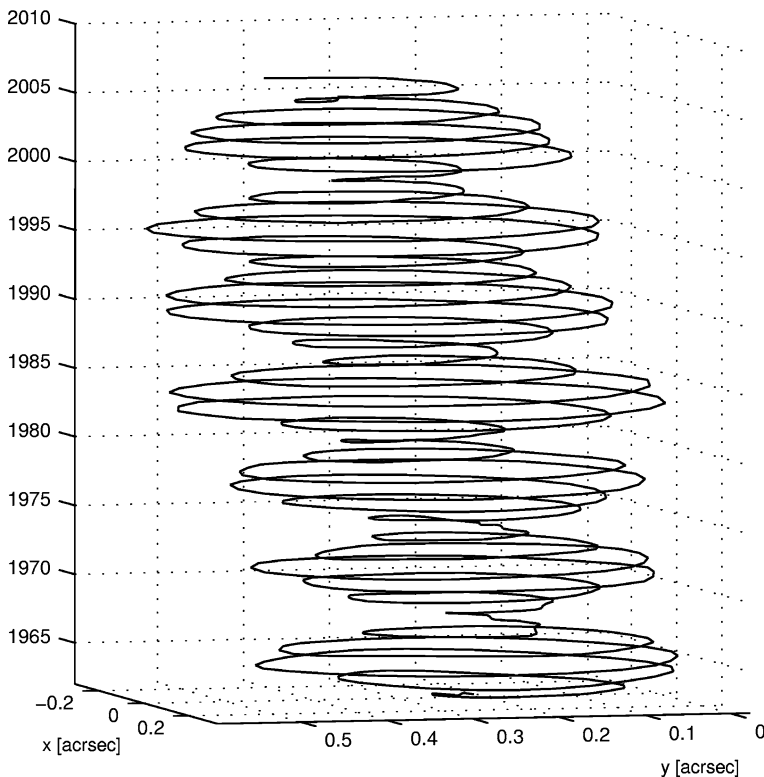


Fig. 1.16 Polar motion plotted with the IERS pole coordinates from 1962 to 2008 as published by the International Earth Rotation and Reference Systems Service on the internet

effect of earthquakes on the Chandler wobble is discussed in literature but is not proven up to now.

- An annual period is superimposed on the Chandler wobble with amplitudes of 0.05" to 0.1" and is caused by seasonal variations in the atmosphere and in the oceans.
- A secular motion of the North Pole is directed to the 70°W meridian with a magnitude of about 0.003" (0.1 m) per year (Fig. 1.17). The postglacial land uplifts in northern Canada and Europe are assumed to be the main causes for the pole drift presently. In addition, the lithosphere plates move horizontally against each other on the less viscous asthenosphere (plate tectonics) which appears as a pole drift (polar wander).

The interaction between Earth rotation and global geodynamical processes is comprehensively explained in Schuh et al. (2003). The superposition of Chandler and annual period induces a modulation (beating) period of 6 years which is clearly seen in Fig. 1.16.

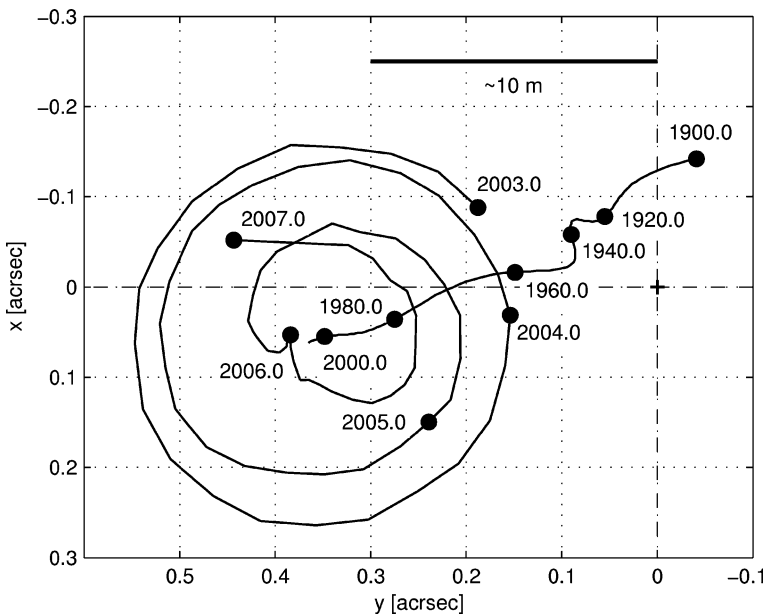


Fig. 1.17 Polar motion 2003–2007 and mean yearly motion calculated for the time points 1,900.0–2,000.0 as viewed from the North Pole (pole coordinates provided by IERS)

The variations of the Earth’s rotation vector change the centrifugal acceleration at any measuring point on the Earth’s surface. For station Hannover ($\phi = 52.44^\circ\text{N}$, $\lambda = 9.71^\circ\text{E}$) the gravity effects are normally within $\pm 5 \mu\text{Gal}$, but attained a maximum of $+7.3$ and a minimum of $-8.6 \mu\text{Gal}$ around 1950. From Fig. 1.17 it becomes obvious that nowadays and in the future the polar motion effect for stations located along the positive direction of the y -axis (North and South America) would be obtained with a positive sign.

The polar motion reduction (Wahr 1985) for absolute gravimetry measurements are given as

$$\Delta g_{\text{pol}} = -\delta_{\text{pol}} \omega^2 r \sin 2\varphi (x_p \cos \lambda - y_p \sin \lambda), \tag{28}$$

with the Earth’s angular velocity ω and radius r , and the geographical latitude φ and longitude λ of the measuring position. The amplitude factor δ_{pol} considers the elastic response of the solid Earth as compared to a rigid Earth’s body. As for the Earth tide amplitudes in the past, the factor 1.16 is applied here for the lack of better knowledge. The daily pole coordinates x_p and y_p of IERS (Bulletin A) are provided as predicted values, which can be used during the online data evaluation of absolute gravity measurements, and as finals which improve the gravity results by post-processing. The high accuracy of the IERS coordinates ($\pm 0.0003''$, Reigber and Feissel 1997) keeps the residual error of this reduction below $0.1 \mu\text{Gal}$ (Timmen

1994). The position coordinates are required with an accuracy of a few kilometres only.

1.5.3 Atmospheric Mass Movements

Gravity variations due to atmospheric mass variations may be subdivided into a direct effect of air mass attraction and an indirect (loading) effect due to the deformation of the Earth's crust and the sea surface. The surface deformation at the gravimeter site can be more than 1 cm. The variations in the local gravity acceleration and atmospheric pressure are known to be correlated with an admittance of -0.3 to $-0.4 \mu\text{Gal/hPa}$ depending on the local, regional and global weather situation (air mass distribution) and on the location of the gravimetry station, e.g. vicinity of the sea. During relative and absolute gravity measurements, the local air pressure is observed to reduce the atmospheric effect from the gravity results. In accordance with the IAG resolution No. 9, 1983 (IGC 1988), the factor $\alpha = -0.3 \mu\text{Gal/hPa}$ should be applied as a global mean if no better information is available. The reduction formula

$$\Delta g_{\text{air}} = -\alpha (p - p_n)[\text{hPa}] \quad (29)$$

refers the actual atmospheric pressure p to the normal atmospheric pressure p_n which is defined by

$$p_n = 1013.25 \left(1 - \frac{0.0065 H_{[m]}}{288.15} \right)^{5.2559} [\text{hPa}] . \quad (30)$$

The reduction applies the US Standard Atmosphere, 1976, as a reference atmospheric model. The station height H (above sea level) should be introduced with an accuracy of better than 10 m for precise absolute gravity determinations.

Absolute gravimetry is more sensitive to atmospheric variations than relative gravimetry because of the short time intervals between two successive relative readings of a gravity difference. Assuming an air pressure variation of more than 30 hPa, the actual coefficient α should be known with an accuracy of better than 5% to ensure a reduction uncertainty of less than $0.5 \mu\text{Gal}$. But that requirement can often not be fulfilled especially when just using the general factor $-0.3 \mu\text{Gal/hPa}$.

At IfE, a more accurate reduction is applied for all FG5 measurements performed in the Fennoscandian land uplift project since 2003. The attraction and deformation effects for a local (spherical distance $\leq 0.5^\circ$), regional ($0.5-10^\circ$) and global ($10-180^\circ$) zone with corresponding resolutions of 0.005° , 0.1° and 1.125° are calculated. The global data are available from the European Centre for Medium-Range Weather Forecasts (ECMWF) and are provided to IfE by the University of Cologne in cooperation with the German Computing Centre for Climate and Earth System Research. The calculation procedure is explained in Gitlein and Timmen (2006).

This improved reduction for absolute gravity measurements with global atmospheric weather data is very costly in terms of labour and needs the development of gravimetric software which is not available in the open market. An improvement of 0.5–1 μGal can be expected (Gitlein 2009) but a residual error in the order of 0.5 μGal can still not be excluded for all gravimetric station determination.

1.5.4 Groundwater Variations

Gravity changes caused by groundwater variations are predominantly a direct gravitational effect of the water masses. Smaller indirect effects are accompanied with a vertical displacement of the measuring position: elastic deformation of the crust due to the water load and sediment consolidation due to a decrease in the water table level and a consequent decline of the pore volume (Romagnoli et al. 2003). Such effects can partly be avoided by selecting stations in mountain areas and bedrock. Temporary water storage is still possible in clefts, crevasses and pockets but the void volume should be much less than 5%, whereas in glacial sediment layers the free volume might be more than 30%. In general, a seasonal behaviour of the groundwater table becomes visible in continuous registrations of water depth gauges. Hence it might be helpful to perform absolute gravity measurements always in the same season of a year to determine secular gravity changes.

For regions with homogeneous sediment layers, a Bouguer-plate model often gives a first approximation for the dependency between changes in gravity and water table readings (Torge 1993):

$$\Delta g_{\text{gw}} = 2\pi G \rho_w P \delta H = 42 P \delta H_{[m]} \quad [\mu\text{Gal}], \quad (31)$$

where G is the gravitational constant and ρ_w is the water density which is 1,000 kg/m^3 . Assuming a pore volume of 30% in the sediment layer ($P = 0.30$) and a water table shift δH of 1 m, a gravity effect of 12.6 μGal is obtained.

For the absolute reference station Hannover, a vertical sediment profile was determined from the drilling of the water gauge close to the gravimetry laboratory. It revealed an average pore volume of 38%. Modelling the change of the groundwater table with a tilted plane (0.4% to the receiving river) and a mean water level depth of 3.7 m, an admittance factor of 15 $\mu\text{Gal/m}$ was derived (Timmen 1994). A similar relation is obtained from the statistical correlation of the water table readings with the absolute gravity measurements performed with the Hannover FG5 meter since 2003 (Sect. 1.6.1). The resulting regression factor with 17 $\mu\text{Gal/m}$ considers not only the primarily affecting Newtonian attraction but also the indirect effects accompanied with a vertical position shift (load and sediment consolidation).

Successful experiments and modelling of gravity effects due to soil moisture and groundwater changes were already described in Mäkinen and Tattari (1988). But, in general, a reduction for hydrological variations is still not applied in absolute and relative gravimetry.

1.6 Gravity Changes: Examples

Some examples for gravimetric applications of IfE are given in Torge (1993) describing projects in tectonically active areas in northern Iceland, the Venezuelan Andes and in the Yunnan (China) earthquake study area. Gitlein et al. (2008) describe the gravimetric survey of the Fennoscandian postglacial rebound which is an isostatic uplift of the Earth’s crust due to the melting of the ice sheet after the glacial maximum of the last ice age. The IfE gravimetry projects in the Nordic countries are all part of a long-term survey task. In close cooperation with the national Nordic surveying agencies and research institutions, IfE has performed gravity observations in Scandinavia since 1986. The monitoring of crustal deformations in northern Europe is still the main focus of the ongoing cooperations.

As already mentioned in Sect. 1.2.2, an important future application may be the monitoring of changes in the hydrosphere, especially if such variations mean some serious consequences for the water supply. To demonstrate the potential of gravimetry as a tool for groundwater monitoring, the situation in Hannover is presented as an example.

1.6.1 Hydrology: Groundwater Variations in Hannover

Figure 1.18 shows the time series of absolute gravity determinations in Hannover (point 103) observed with the two Hannover instruments. The station is located on glacial sediments with a thickness of about 500 m (sand, clay and marl of low consolidation). The free-fall experiments are severely affected by natural (wind forces on the adjacent buildings) and man-made (machines, traffic) seismic noise. The history of the Hannover measurements reveals a linear gravity decrease of about 25 μGal over a period of 21 years, whereas in Clausthal (Fig. 1.6) no significant secular gravity variation can be found. An explanation for the phenomenon in Hannover is not yet available and requires discussions with other experts, e.g. from hydrosphere research. Figure 1.19 illustrates the scatter in the time histories which is not

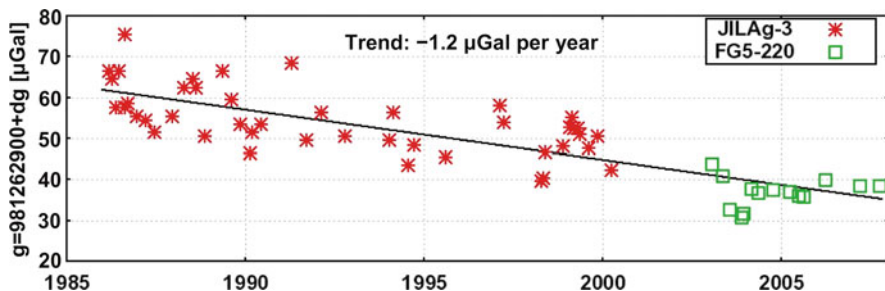


Fig. 1.18 Absolute gravity determinations with JILAg-3 (offset corrected) and FG5-220 at stations Hannover (HAN103, trend $-1.2 \pm 0.1 \mu\text{Gal}/\text{year}$)

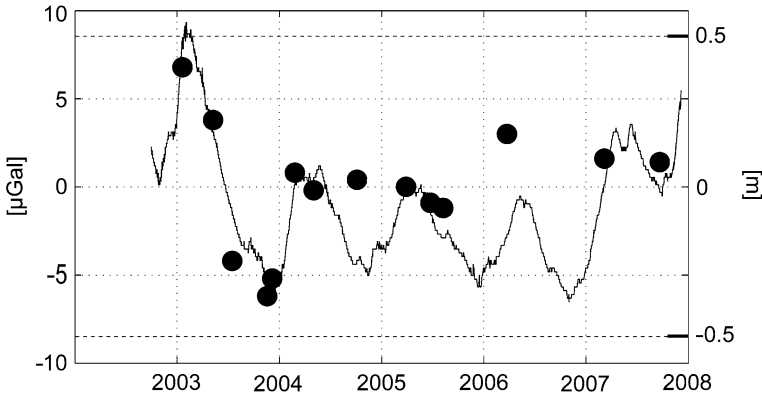


Fig. 1.19 Groundwater table at the gravimetry laboratory in Hannover and absolute gravity determinations with FG5-220 since 2003. The transfer function from gravity to groundwater change, with the linear coefficient $17 \mu\text{Gal}/\text{m}$ (correlation 80%), has been applied to the absolute gravity determinations to convert the g -values to groundwater readings

only caused by measurement uncertainties but also by real gravity variations. For example, from February to December 2003 the groundwater table at the gravimetry laboratory in Hannover fell about 70 cm due to the very dry season in northern Germany. This was accompanied by a gravity decrease of $13 \mu\text{Gal}$. Checking the groundwater readings for the period 1986 to the present, a declining trend over the years is not visible. But these readings from the groundwater gauge consider only the upper aquifer of the subsurface hydrology around the gravimetry laboratory and not the deeper aquifers. Thus, it cannot be excluded that the long-term trend in the gravity series might be caused by a change in the subsurface water content.

1.6.2 Tectonics: Isostatic Land Uplift in Fennoscandia

In the Fennoscandian land uplift area, the Earth's crust has been rising continuously since the last glacial maximum in response to the deloading of the ice. This process is an isostatic adjustment of the Earth's elastic lithosphere and underlying viscous mantle. For a general overview Wolf (1993) gives a historical review about the changing role of the lithosphere in models of glacial isostasy.

The Fennoscandian rebound area is dominated by the Precambrian basement rocks of the Baltic Shield, which is part of the ancient East European Craton and comprises south Norway, Sweden, Finland, the Kola Peninsula and Russian Karelia. The region is surrounded by a flexural bulge, covering northern Germany and northern Poland, the Netherlands and some other surrounding regions. The bulge area was once rising due to the Fennoscandian ice load and, after the melting, sinking with a much smaller absolute value than the uplift rate in the centre of Fennoscandia. Denmark is part of the transition zone from the uplift to the subsidence area. The maximum spatial extension of the uplift area is about 2,000 km in northeast–southwest direction; see Fig. 1.20 for the approximate shape (after Ågren

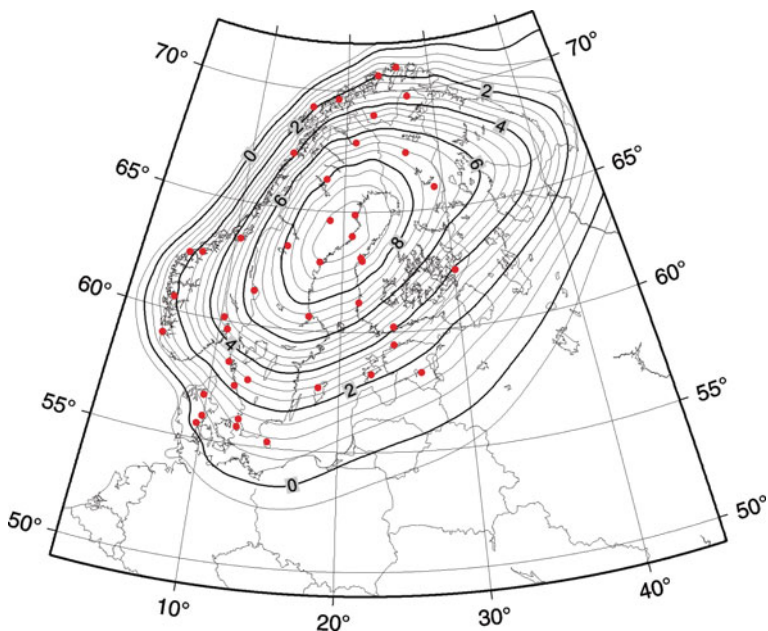


Fig. 1.20 Map of the postglacial uplift of Fennoscandia in mm/year after Ågren and Svensson (2007) derived from model NKG2005LU, courtesy of Ågren. The dots indicate the positions of gravity stations of the Nordic Absolute Gravity Project

and Svensson 2007). Presently, the central area around the northern part of the Gulf of Bothnia is undergoing an uplift at a rate of about 1 cm/year.

The Trans-European Suture Zone (TESZ) is a main tectonic boundary in Europe, separating the East European Craton from the Phanerozoic terrains in the west and southwest (Palaeozoic western Europe and Meso-Europe). The Sorgenfrei-Tornquist Zone is part of the TESZ and crosses Denmark north of Copenhagen in the immediate vicinity of the absolute gravity station Helsingør; see Fig. 1.10 for the station names and locations. Among other stations, the absolute gravity stations Copenhagen/Vestvolden, Helsingør, Onsala and Borås belong to the Nordic Geodetic Observing System (NGOS) and constitute the central part of a north–south profile crossing perpendicularly the graben system of the suture zone between the Baltic Shield and the younger Palaeo-Europe.

Four east–west profiles across the Fennoscandian postglacial rebound area have been utilised by relative gravimetry and levelling. They follow approximately the latitudes 65°N (observed 1975–2000), 63°N (1966–2003), 61°N (1976–1983) and 56°N (1977–2003); see Ekman and Mäkinen (1996) or Mäkinen et al. (2004). The east–west directions were chosen to ensure only small gravity differences between the relative gravimetry points (less than 1 mGal). This requirement avoids errors from uncertainties of the gravimeter calibrations. With the availability of transportable absolute gravimetry in Central Europe, the 56° profile (Denmark–Sweden) was supported with JILAg-3 (in 1986) and FG5-220 (2003, 2005) measurements.

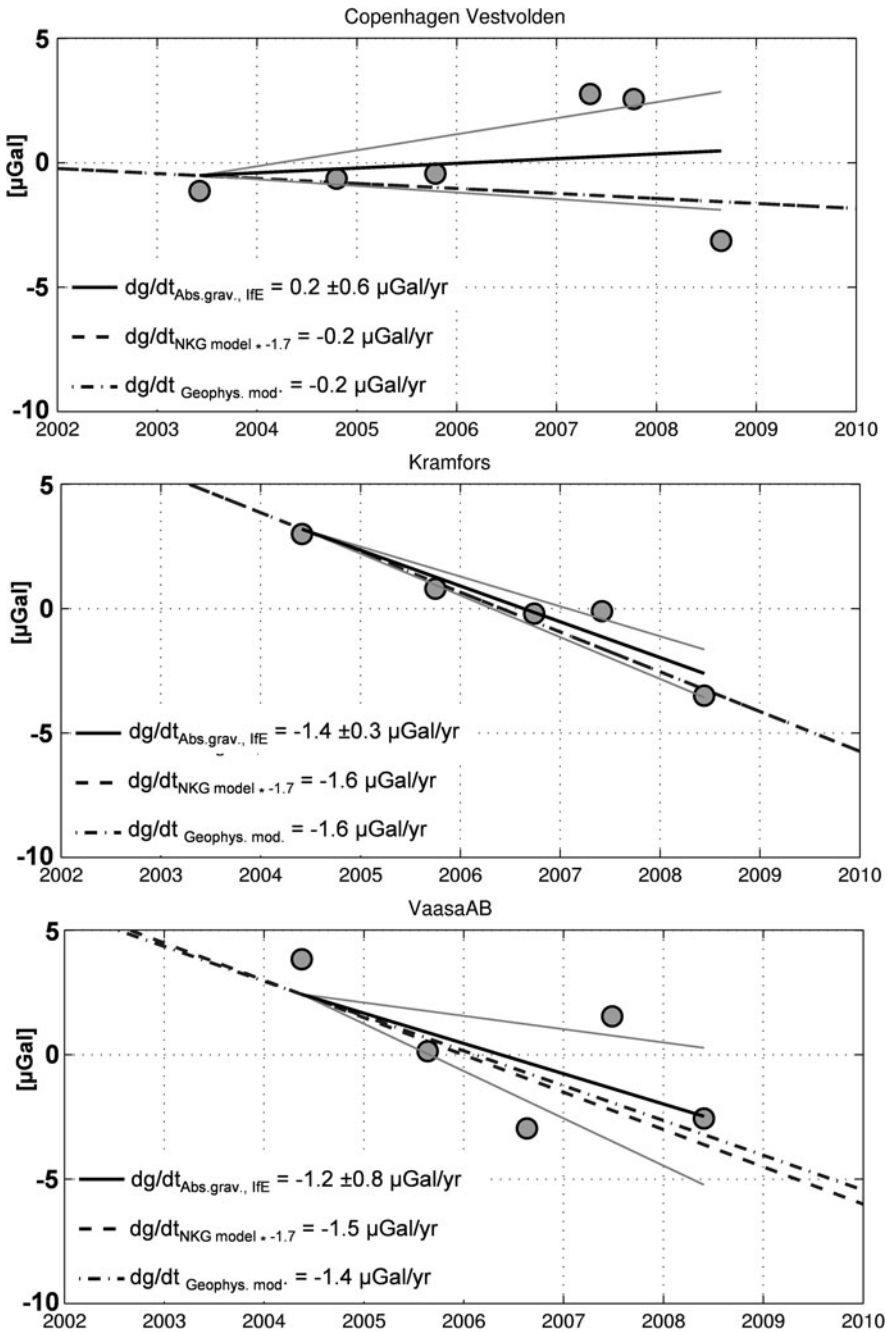


Fig. 1.21 Linear gravity changes for three stations in Fennoscandia derived from absolute gravity measurements of IfE and compared with the trends from the NKG2005LU model (Fig. 1.20, conversion factor $-1.7 \mu\text{Gal/cm}$ applied) and from the model predictions provided by Klemann (2004). The *grey lines* beside the IfE trends indicate the standard deviation of the corresponding trend line

Repeated observations with the FG5-220 from IfE were performed at 11 stations in Fennoscandia nearly every year from 2003 to 2008 (Gitlein et al. 2008). From these results, linear gravity changes were calculated for each station (Gitlein 2009). The trends for three stations are presented exemplarily in Fig. 1.21. A decrease in gravity due to land uplift is evident at almost all stations. The largest gravity changes were found around the uplift centre (e.g. Kramfors). In Copenhagen, close to the zero uplift line in Fig. 1.20, the obtained gravity rate is nearly zero. Overall, the regional rebound signal is clearly visible, but still seems to be disturbed by environmental mass variations, e.g. at station VaasaAB. From the experiences over the last 5 years, the hydrological changes are considered as a main contributor, which is also indicated by the water level observations of the reservoirs and wells close to some of the absolute stations.

In Fig. 1.21 the observational trends are compared with the results derived from the NKG2005LU model (Ågren and Svensson 2007), which is mainly based on levelling and GPS results, and with predicted rates of a glacial rebound model provided by Klemann (2004). The computations were based on solution algorithms developed by Martinec (2000) and Hagedoorn et al. (2007) and use a global ice model with SCAN-II (Lambeck et al. 1998) for Fennoscandia. Overall, the trends observed by absolute gravimetry since 2003 or 2004 are in good agreement with the other results. The obtained standard deviations seem to be realistic estimates for the accuracy of the deduced secular gravity changes. The disturbances caused by unaccounted hydrological effects are cancelled out in the trends to some extent due to the annual gravity measurements. Thus, absolute gravimetry has shown its capability to observe the Fennoscandian land uplift within the rather short time span of 4–5 years.

References

- Agnew, D.C. (1997) NLOADF: a program for computing ocean-tide loading. *J. Geophys. Res.*, 102(B3), 5109–5110
- Ågren, J. and Svensson, R. (2007) Postglacial land uplift model and system definition for the new Swedish height system RH 2000. Reports in Geodesy and Geographical Information Systems, Lantmateriet, Gävle, 123 pp
- Bilker-Koivula, M., Mäkinen, J., Timmen, L., Gitlein, O., Klopping, F. and Falk, R. (2008) Repeated absolute gravity measurements in Finland. In: Peshekhonov, V.G. (ed) *Terrestrial Gravimetry: Static and Mobile Measurements (TG-SMM2007)*. Proceedings of International Symposium, Elektropribor, St. Petersburg, pp. 147–151
- BIPM (2006) Bureau international des poids et mesures, *Le Système international d'unités (SI) – The International System of Units (SI)*. 8e édition, 2006. Édité par le BIPM, Pavillon de Breteuil, F-92312 Sèvres Cedex, France
- Boedecker, G. and Flury, J. (1995) International Absolute Gravity Basestation Network IAGBN, Catalogue of stations and observations. Report of the IAG International Gravity Commission, IGC-Working Group 2, “World Gravity Standards”, available at the Bureau Gravimetrique International, Toulouse
- Boedecker, G. and Fritzer, Th. (1986) International Absolute Gravity Basestation Network. Veröff. Bayer. Komm. für die Internat. Erdmessung der Bayer. Akad. d. Wissensch., Astron.-Geod. Arb. 47, München

- Boulanger, Yu., Faller, J., Groten, E., Arnautov, G., Becker, M., Bernard, B., Cannizzo, L., Cerutti, G., Courtier, N., Feng Youg-Yuan, Friederich, J., Guo You-Guang, Hanada, H., Huang Da-Lun, Kalish, E., Klopping, F., Li De-Xi, Liard, J., Mäkinen, J., Marson, I., Ooe, M., Peter, G., Röder, R., Ruess, D., Sakuma, A., Schnüll, M., Stus, F., Scheglov, S., Tarasuk, W., Timmen, L., Torge, W., Tsubokawa, T., Tsuruta, S., Vänskä, A. and Zhang Guang-Yuan (1991) Results of the 3rd International Comparison of Absolute Gravimeters in Sèvres 1989. *Bur. Grav. Int., Bull. d'Inf.*, 68, 24–44, Toulouse
- Carter, W.E., Aubrey, D.G., Baker, T., Boucher, C., LeProvost, C., Pugh, D., Peltier, W.R., Zumbege, M., Rapp, R.H., Schutz, R.E., Emery, K.O. and Enfield, D.B. (1989) Geodetic fixing of tide gauge bench marks. Woods Hole Oceanographic Institution Report WHOI-89-31/CRC-89-5, Woods Hole
- Carter, W.E., Peter, G., Sasagawa, G.S., Klopping, F.J., Berstis, K.A., Hilt, R.L., Nelson, P., Christy, G.L., Niebauer, T.M., Hollander, W., Seeger, H., Richter, B., Wilmes, H. and Lothammer, A. (1994) New gravity meter improves measurements. *EOS, Trans. Am. Geophys. Union*, 75(08), 90–92
- Cartwright, D.E. and Edden, A.C. (1973) Corrected tables of tidal harmonics. *Geophys. J. R. Astr. Soc.*, 33, 253–264
- Cartwright, D.E. and Tayler, R.J. (1971) New computations of the tide-generating potential. *Geophys. J. R. Astr. Soc.*, 23, 45–74
- Cook, A.H. (1965) The absolute determination of the acceleration due to gravity. *Metrologia*, 1, 84–114
- Dehant, V. (1987) Tidal parameters for an inelastic Earth. *Phys. Earth Planet. Inter.*, 49, 97–116
- Doodson, A.T. (1921) The harmonic development of the tide-generating potential. *Proc. R. Soc. (London)*, Series A 100, 306–328. Reprint in *Int. Hydrographic Revue* 31, Monaco 1954
- Dziewonski, A.M. and Anderson, D.L. (1981) Preliminary reference earth model (PREM). *Phys. Earth Planet. Int.*, 25, 297–356
- Ekman, M. and Mäkinen, J. (1996) Recent postglacial rebound, gravity change and mantle flow in Fennoscandia. *Geophys. J. Int.*, 126, 229–234
- Everaerts, M., Lambot, Ph., Van Hoolst, T., van Ruymbeke, M. and Ducarme, B. (2002) First order gravity network of Belgium. *Bur. Grav. Int., Bull. d'Inf.*, 90, 27–42, Toulouse
- Falk, R. (1995) Erste Erfahrungen mit dem Automatischen Gravimeter Scintrex CG-3 M Autograv. *Zeitschrift für Vermessungswesen*, Verlag Wittwer, Stuttgart, Heft 1, 26–34
- Faller, J.E., Guo, Y.G., Geschwind, J., Niebauer, T.M., Rinker, R.L. and Xue, J. (1983) The JILA portable absolute gravity apparatus. *Bur. Grav. Int., Bull. d'Inf.*, 53, 87–97, Toulouse
- Francis, O. and van Dam, T. (2006) Analysis of results of the International Comparison of Absolute Gravimeters in Walferdange (Luxembourg) of November 2003. *Cahiers du Centre Européen de Géodynamique et de Séismologie*, 26, 1–23, Luxembourg
- Francis, O., van Dam, T., Germak, A., Amalvict, M., Bayer, R., Bilker-Koivula, M., Calvo, M., D'Agostino, G.-C., Dell'Acqua, T., Engfeldt, A., Faccia, R., Falk, R., Gitlein, O., Fernandez, Gjevestad, J., Hinderer, J., Jones, Kostelecky, J., Le Moigne, N., Luck, B., Mäkinen, J., McLaughlin, D., Olszak, T., Olsson, P., Pachuta, A., Palinkas, V., Pettersen, B., Pujol, R., Prutkin, I., Quagliotti, D., Reudink, R., Rothleitner, C., Ruess, D., Shen, C., Smith, V., Svitlov, S., Timmen, L., Ulrich, C., Van Camp, M., Walo, J., Wang, L., Wilmes, H. and Xing, L. (2010) Results of the European Comparison of Absolute Gravimeters in Walferdange (Luxembourg) of November 2007. *Proceedings of the IAG Symposium on Gravity, Geoid and Earth Observations 2008*, Chania, Crete, Greece, June 2008, Springer (accepted for publication)
- Gitlein, O. (2009) *Absolutgravimetrische Bestimmung der Fennoskandischen Landhebung mit dem FG5-220*. Dissertation, Wissenschaftliche Arbeiten der Fachrichtung Geodäsie und Geoinformatik der Leibniz Universität Hannover (im Review-Prozess)
- Gitlein, O. and Timmen, L. (2006) Atmospheric mass flow reduction for terrestrial absolute gravimetry in the Fennoscandian land uplift network. In: Tregoning, P. and Rizos, C. (eds) *Dynamic Planet. IAG Symposium 130*, Springer, Berlin, pp. 461–466

- Gitlein, O., Timmen, L., Müller, J., Denker, H., Mäkinen, J., Bilker-Koivula, M., Pettersen, B.R., Lysaker, D.I., Svendsen, J.G.G., Wilmes, H., Falk, R., Reinhold, A., Hoppe, W., Scherneck, H.-G., Engen, B., Omang, O.C.D., Engfeldt, A., Lilje, M., Strykowski, G. and Forsberg, R. (2008) Observing absolute gravity acceleration in the Fennoscandian land uplift area. In: Peshekhonov, V.G. (ed) *Terrestrial Gravimetry: Static and Mobile Measurements (TG-SMM2007)*. Proceedings of the International Symposium. Elektropribor, St. Petersburg, pp. 175–180
- Hagedoorn, J.M., Wolf, D. and Martinec, Z. (2007) An estimate of global mean sea-level inferred from tide-gauge measurements using glacial-isostatic models consistent with the relative sea-level record. *Pure Appl. Geophys.*, 164, 791–818, Birkhäuser Verlag, Basel
- Hartmann, T. and Wenzel, H.-G. (1995) The HW95 tidal potential catalogue. *Geophys. Res. Lett.*, 22, 3553–3556
- Hugill, A.L. (1988) The new Scintrex CG-3 Automated Gravity Meter: description and test results. Paper presented at the ASEG/SEG Conference, February 1988. Adelaide
- IGC (1988) International Absolute Gravity Basestation Network (IAGBN), Absolute Gravity Observations, Data Processing Standards & Station Documentation (Int. Grav. Com. -WGII: World Gravity Standards). *Bur. Grav. Int., Bull. d'Inf.*, 63, 51–57, Toulouse
- Ilk, K.H., Flury, J., Rummel, R., Schwintzer, P., Bosch, W., Haas, C., Schröter, J., Stammer, D., Zehel, W., Miller, H., Dietrich, R., Huybrechts, P., Schmeling, H., Wolf, D., Götze, H.J., Riegger, J., Bardossy, A., Güntner, A. and Gruber, Th. (2005) Mass transport and mass distribution in the Earth system – Contribution of the new generation of satellite gravity and altimetry missions to geosciences. GOCE Projektbüro, TU München und GFZ Potsdam
- Jentzsch, G. (1997) Earth tides and ocean tidal loading. In: Wilhelm, H., Zürn, W. and Wenzel, H.-G. (eds) *Tidal Phenomena. Lecture Notes in Earth Sciences*, Vol. 66. Springer, Heidelberg, pp. 145–171
- Jentzsch, G. (2008) The automated Burris Gravity Meter – a new instrument using an old principle. In: Peshekhonov, V.G. (ed) *Terrestrial Gravimetry: Static and Mobile Measurements (TG-SMM2007)*. Proceedings of the International Symposium. Elektropribor, St. Petersburg, pp. 21–28
- Jousset, M., van Ruymbeke, M., Bonvalot, S. and Diament, M. (1995) Performance of two Scintrex CG3M instruments at the Fourth International Comparison of Absolute Gravimeters. *Metrologia*, Sèvres, 32, 231–244
- Kangieser, E., Kummer, K., Torge, W. and Wenzel, H.-G. (1983) Das Gravimeter Eichsystem Hannover. *Wiss. Arb. d. Fachrichtung Verm.wesen der Univ. Hannover*, Nr. 120
- Klemann, V. (2004) Linear gravity variations for the IfE absolute gravity stations in Fennoscandia predicted by geophysical GIA modelling. Personal communication, Deutsches GeoForschungsZentrum (GFZ), Potsdam
- Krieg, L.A. (1981) Mathematical modelling of the behaviour of the LaCoste and Romberg "G" gravity meter for use in gravity network adjustments and data analyses. Reports of the Department of Civil and Environmental Engineering and Geodetic Science, Geodetic Science and Surveying, The Ohio State University, Columbus, 321
- Lambeck, K., Smither, C. and Ekman, M. (1998) Tests of glacial rebound models for Fennoscandia based on instrumented sea- and lake-level records. *Geophys. J. Int.*, 135, 375–387
- Lambert, A., Courtier, N., Sasagawa, G.S., Klopping, F., Winester, D., James, T.S. and Liard, J.O. (2001) New constraints on Laurentide Postglacial rebound from absolute gravity measurements. *Geophys. Res. Lett.*, 28, 2109–2211
- Lambert, A., James, T.S., Liard, J.O. and Coutier, N. (1996) The role and capability of absolute gravity measurements in determining the temporal variations in the earth's gravity field. *IAG Symposium 116*. Springer, Berlin, pp. 20–29
- Liard, J. and Gagnon, C. (2002) The new A-10 absolute gravimeter at the 2001 International Comparison of Absolute Gravimeters. *Metrologia*, 39, 477–483
- Mäkinen, J., Amalvict, M., Shibuya, K. and Fukuda, Y. (2007) Absolute gravimetry in Antarctica: status and prospects. *J Geodynamics*, 43, 339–357

- Mäkinen, J., Engfeldt, A., Harrison, B.G., Ruotsalainen H., Strykowski, G., Oja, T. and Wolf, D. (2004) The Fennoscandian Land Uplift Gravity Lines 1966–2003. Proceedings (CD publ.) of the IAG Symposium Gravity, Geoid and Space Missions (GGSM2004), Porto, 2004
- Mäkinen, J. and Tattari, S. (1988) Soil moisture and groundwater: two sources of gravity variations. *Bur. Grav. Int., Bull. d'Inf.*, 62, 103–110, Toulouse
- Marson, I., Faller, J.E., Cerutti, G., De Maria, P., Chartier, J.-M., Robertsson, L., Vitushkin, L., Friederich, J., Krauterbluth, K., Stizza, D., Liard, J., Gagnon, C., Lothhammer, A., Wilmes, H., Mäkinen, J., Murakami, M., Rehren, F., Schnüll, M., Ruess, D. and Sasagawa, G.S. (1995) Fourth international comparison of absolute gravimeters. *Metrologia*, 32, 137–144
- Martinec, Z. (2000) Spectral-finite element approach to three-dimensional viscoelastic relaxation in a spherical earth. *Geophys. J Int*, 142, 117–141
- Micro-g Solutions Inc. (1999) Operator's manual, FG5 absolute gravimeter. Micro-g Solutions Inc, Erie
- Müller, J., Neumann-Redlin, M., Jarecki, F., Denker, H. and Gitlein, O. (2006) Gravity changes in northern Europe as observed by GRACE. In: Tregoning, P. and Rizos, C. (eds) *Dynamic Planet. IAG Symposium 130*. Springer, Berlin, pp. 523–257
- Nagorny, V.D. (1995) A new approach to absolute gravimeter analysis. *Metrologia*, 32, 201–208
- Niebauer, T.M. (1987) New absolute gravity instruments for physics and geophysics. Ph.D. thesis, University of Colorado, Department of Physics, Boulder
- Niebauer, T.M., Klopping, F.G., Bilson, R. and Brown, J.M. (1999) The new A10 absolute field gravimeter. *EOS Trans. AGU*, 80(17), Spring Meet. Suppl. S85
- Niebauer, T.M., Sasagawa, G.S., Faller, J.E., Hilt, R. and Klopping, F. (1995) A new generation of absolute gravimeters. *Metrologia*, 32, 159–180
- Pearlman, M., Altamini, Z., Beck, N., Forsberg, R., Gurtner, W., Kenyon, S., Behrend, D., Lemoine, F.G., Ma, C., Noll, C.E., Pavlis, E.C., Malkin, Z., Moore, A.W., Webb, F.H., Neilan, R.E., Ries, J.C., Rothacher, M. and Willis, P. (2006) GGOS working group on ground networks and communications. In: Tregoning, P. and Rizos, C. (eds) *Dynamic Planet. IAG Symposium, 130*, Springer, Berlin, pp. 719–726
- Rapp, R.H. (1983) Tidal gravity computations based on recommendations of the Standard Earth Tide Committee. *Bull. d'Inf., Marées Terrestres*, 89, 5814–5819, Bruxelles
- Rehren, F. (1997) Relative gravity measurements with a Scintrex CG-3 M in the Gravimeter Calibration Systems Hannover and Hornisgrinde. *Bur. Grav. Int., Bull. d'Inf.*, 81, 23–29, Toulouse
- Reigber, C. and Feissel, M. (1997) IERS missions, present and future. Report on the 1996 IERS Workshop. IERS Technical Note 22, Paris
- Robertsson, L., Francis, O., vanDam, T.M., Faller, J., Ruess, D., Delinte, J.-M., Vitushkin, L., Liard, J., Gagnon, C., Guo You Guang, Huang Da Lun, Fang Yong Yuan, Xu Jin Yi, Jeffries, G., Hopewell, H., Edge, R., Robinson, I., Kibble, B., Mäkinen, J., Hinderer, J., Amalvict, M., Luck, B., Wilmes, H., Rehren, F., Schmidt, K., Schnüll, M., Cerutti, G., Germak, A., Zabek, Z., Pachuta, A., Arnaudov, G., Kalish, E., Stus, Y., Stizza, D., Friederich, J., Chartier, J.-M. and Marson, I. (2001) Results from the Fifth International Comparison of Absolute Gravimeters, ICAG97. *Metrologia*, 38, 71–78
- Röder, R.H., Schnüll, M. and Wenzel, H.-G. (1985) Gravimetry with an electrostatic feedback system. *Bur. Grav. Int., Bull. d'Inf.*, 57, 72–81, Toulouse
- Röder, R.H., Schnüll, M. and Wenzel, H.-G. (1988) SRW feedback for LaCoste-Romberg gravimeters with extended range. *Bur. Grav. Int., Bull. d'Inf.*, 62, 46–50, Toulouse
- Romagnoli, C., Zerbini, S., Lago, L., Richter, B., Simon, D., Domenichini, F., Elmi, C. and Ghirelli, M. (2003) Influence of soil consolidation and thermal expansion effects on height and gravity variations. *J Geodynamics*, 35, 521–539
- Schmerge, D. and Francis, O. (2006) Set standard deviations, repeatability and offset of absolute gravimeter A10-008. *Metrologia*, 43, 414–418
- Schnüll, M., Röder, R.H. and Wenzel, H.-G. (1984) An improved electronic feedback for LaCoste-Romberg gravity meters. *Bur. Grav. Int., Bull. d'Inf.*, 55, 27–36, Toulouse

- Schuh, H., Dill, R., Greiner-Mai, H., Kutterer, H., Müller, J., Nothnagel, A., Richter, B., Rothacher, M., Schreiber, U. and Soffel, M. (2003) Erdrotation und globale dynamische Prozesse. Mitteilungen des Bundesamtes für Kartographie und Geodäsie 32, 118 Seiten, Verlag des Bundesamtes für Kartographie und Geodäsie, Frankfurt a.M.
- Schwiderski, E. (1980) Ocean tides, part I: global ocean tidal equations; part II: a hydrodynamical interpolation model. *Marine Geodesy*, 3, 161–255
- Scintrex (1998) CG-3/3 M Gravity Meter, User's Guide, Concord
- Tamura, Y. (1987) A harmonic development of the tide generating potential. *Bull. d'Inf., Marées Terrestres*, 99, 6813–6855, Bruxelles
- Tapley, B., Bettadpur, S., Ries, J., Thompson, P. and Watkins, M. (2004) GRACE measurements of mass variability in the Earth System. *Science*, 305, 503–505
- Timmen, L. (1994) Untersuchungen zur Modellbildung bei der Auswertung absoluter Schweremessungen. *Wiss. Arb. d. Fachrichtung Verm.wesen der Univ. Hannover*, 204, Dissertation am Institut für Erdmessung, Universität Hannover
- Timmen, L. (1996) Absolutgravimetrie – Aufgaben und Anwendungen. *Zeitschrift für Vermessungswesen (ZfV)* 121, 286–295, Wittwer, Stuttgart
- Timmen, L. (2003) Precise definition of the effective measurement height of free-fall absolute gravimeters. *Metrologia*, 40, 62–65
- Timmen, L., Flury, J., Peters, T. and Gitlein, O. (2006a) A new absolute gravity base in the German Alps. In: Hvoždara, M. and Kohúh I. (eds) *Contributions to Geophysics and Geodesy, 2nd Workshop on International Gravity Field Research (special issue)* 36, 7–20, Slovak Academy of Sciences, Bratislava
- Timmen, L., Gitlein, O., Müller, J., Denker, H., Mäkinen, J., Bilker, M., Pettersen, B.R., Lysaker, D.I., Omang, O.C.D., Svendsen, J.G.G., Wilmes, H., Falk, R., Reinhold, A., Hoppe, W., Scherneck, H.-G., Engen, B., Harsson, B.G., Engfeldt, A., Lilje, M., Strykowski, G. and Forsberg, R. (2006b) Observing fennoscandian gravity change by absolute gravimetry. In: Sansò, F. and Gil A.J. (eds) *Geodetic Deformation Monitoring: From Geophysical to Engineering Roles. IAG Symposium 131*, Springer, Berlin, Heidelberg, pp. 193–199
- Timmen, L. and Wenzel, H.-G. (1994) Improved gravimetric Earth tide parameters for station Hannover. *Bull. d'Inf., Marées Terrestres*, 119, 8834–8846, Bruxelles
- Timmen, L. and Wenzel, H.-G. (1995) Worldwide synthetic gravity tide parameters. In: Sünkel, H. and Marson, I. (eds) *Gravity and Geoid. Proceedings of IAG Symposium*, 113, Springer, Berlin, Heidelberg, pp. 92–101
- Torge, W. (1989) *Gravimetry*. de-Gruyter, Berlin-New York
- Torge, W. (1990) Absolute gravimetry as an operational tool for geodynamic research. In: Brunner, F.K. and Rizos, C. (eds) *Proceedings of the Ron Mather Symposium on Four-Dimensional Geodesy (Sydney, 1989)*. *Lecture Notes in Earth Sciences*, Vol. 29. Springer, Berlin, pp. 15–28
- Torge, W. (1991) The present state of absolute gravimetry. *Cahiers du Centre Européen de Géodynamique et de Séismologie*, 3, 9–22, Luxembourg
- Torge, W. (1993) Gravimetry and tectonics. *Publications of the Finnish Geodetic Institute (Geodesy and Geophysics)* 115, 131–172, Helsinki
- Torge, W. (1998a) The changing role of gravity reference networks. In: Forsberg, R., Feissel, M. and Dietrich, R. (eds) *Geodesy on the Move. IAG Symposium*, 119, Springer, Berlin, Heidelberg, New York, etc., pp. 1–10
- Torge, W. (1998b) 100 Jahre Schwerereferenznetze – klassische und moderne Konzeption. *Zeitschrift für Vermessungswesen (ZfV)*, 123, 355–363, Wittwer, Stuttgart
- Torge, W., Falk, R., Franke, A., Reinhart, E., Richter, B., Sommer, M. and Wilmes, H. (1999) Das Deutsche Schweregrundnetz 1994 (DSGN94). DGK, B 309, München
- Torge, W., Röder, R.H., Schnüll, M., Wenzel, H.-G. and Faller, J.E. (1987) First results with the transportable absolute gravity meter JILAg-3. *Bull. Géod.*, 61(2), 161–176, Springer, Berlin – Heidelberg
- Wahr, J.M. (1981) Body tides on an elliptical, rotating, elastic and oceanless Earth. *Geophys. J. Royal Astron. Soc.*, 64, 677–703, Oxford

- Wahr, J. (1985) Deformation induced by polar motion. *J. Geophys. Res.*, 92(B2), 1281–1286
- Wahr, J. and Velicogna, I. (2003) What might GRACE contribute to studies of post glacial rebound. *Space Sci. Rev.*, 108, 319–330
- Wang, R. (1997) Tidal response of the solid Earth. In: Wilhelm, H., Zürn, W. and Wenzel, H.-G. (eds) *Tidal Phenomena. Lecture Notes in Earth Sciences*, Vol. 66, Springer, Heidelberg, pp. 27–57
- Wenzel, H.-G. (1993) Programmsystem GRAV, programme manual, Geodetical Institute University of Karlsruhe, Karlsruhe
- Wenzel, H.-G. (1997) Tide-generating potential for the Earth. In: Wilhelm, H., Zürn, W. and Wenzel, H.-G. (eds) *Tidal Phenomena. Lecture Notes in Earth Sciences*, Vol. 66. Springer, Heidelberg, pp. 9–26
- Williams, S.D.P., Baker, T.F. and Jeffries, G. (2001) Absolute gravity measurements at UK tide gauges. *Geophys. Res. Lett.*, 28, 2317–2329.
- Wilmes, H. and Falk, R. (2006) Bad Homburg – a regional comparison site for absolute gravity meters. *Cahiers du Centre Européen de Géodynamique et de Séismologie*, 26, 29–30, Luxembourg
- Wolf, D. (1993) The changing role of the lithosphere in models of glacial isostasy: a historical review. *Global Planetary Change*, 8, 95–106, Elsevier Science Publishers B.V., Amsterdam
- Xu, J., Zhu, S., Lui, X., Torge, W., Röder, H., Schnüll, M. and Wenzel, H.-G. (1988) Vertical Gravimeter Calibration Line Wuhan/China. *Bur. Grav. Int., Bull. d'Inf.*, 62, 119–125, Toulouse
- ZLS Corporation (2007) User guide: Automated Burris Gravity MeterTM and UltraGravTM Control System, 67pp
- Zürn, W. and Wilhelm, H. (1984) *Tides of the earth*. Landolt-Börnstein, New Series V, 2, 259–299, Springer, Heidelberg-New-York